In vivo time-lapse imaging reveals extensive neural crest and endothelial cell interactions during neural crest migration and formation of the dorsal root and sympathetic ganglia

Lynn George [a,b,*], Haley Dunkel [a], Barbara J. Hunnicutt [a], Michael Filla [c], Charles Little [c], Rusty Lansford [d,e], Frances Lefcort [a]

[a] Department of Cell Biology and Neuroscience, Montana State University, Bozeman, MT 59717, United States
[b] Department of Biological and Physical Sciences, Montana State University Billings, Billings, MT 59101, United States
[c] University of Kansas Medical Center, Kansas City, KS 66160, United States
[d] Department of Radiology and Developmental Neuroscience Program, Saban Research Institute, Children's Hospital Los Angeles, Los Angeles, CA 90027, United States
[e] Keck School of Medicine, University of Southern California, Los Angeles, CA 90033, United States

ARTICLE INFO

ABSTRACT

During amniote embryogenesis the nervous and vascular systems interact in a process that significantly affects the respective morphogenesis of each network by forming a "neurovascular" link. The importance of neurovascular cross-talk in the central nervous system has recently come into focus with the growing awareness that these two systems interact extensively both during development, in the stem-cell niche, and in neurodegenerative conditions such as Alzheimer's Disease and Amyotrophic Lateral Sclerosis. *With respect to the peripheral nervous system, however, there have been no live, real-time investigations of the potential relationship between these two developing systems.* To address this deficit, we used multi-spectral 4D time-lapse imaging in a transgenic quail model in which endothelial cells (ECs) express a yellow fluorescent marker, while neural crest cells (NCCs) express an electroporated red fluorescent marker. We monitored EC and NCC migration in real-time during formation of the peripheral nervous system. Our time-lapse recordings indicate that NCCs and ECs are physically juxtaposed and dynamically interact at multiple locations along their trajectories. These interactions are stereotypical and occur at precise anatomical locations along the NCC migratory pathway. NCCs migrate alongside the posterior surface of developing intersomitic vessels, but fail to cross these continuous streams of motile ECs. NCCs change their morphology and migration trajectory when they encounter gaps in the developing vasculature. Within the nascent dorsal root ganglion, proximity to ECs causes filopodial retraction which curtails forward persistence of NCC motility. Overall, our time-lapse recordings support the conclusion that primary vascular networks substantially influence the distribution and migratory behavior of NCCs and the patterned formation of dorsal root and sympathetic ganglia.

Published by Elsevier Inc. This is an open access article under the CC BY-NC-ND license (http://creativecommons.org/licenses/by-nc-nd/4.0/).

1. Introduction

How a precisely patterned peripheral nervous system (PNS) emerges from a heterogeneous population of neural crest cells remains a fundamental question in developmental biology. Trunk NCCs undergo an epithelial-to-mesenchymal transition to delaminate from the neural tube and then migrate ventrally and laterally through the embryo: those NCCs that stop next to the dorsal aorta differentiate into the paravertebral chain of sympathetic ganglia (SG) while those that stop adjacent to the neural tube give rise to the dorsal root ganglia (DRG) (Lallier and Bronner-Fraser, 1988; Le Douarin and Kalcheim, 1999; Tosney, 1978; Weston, 1970). The cues that guide NCCs to preferentially colonize either the presumptive SG or DRG are not fully understood. NCCs delaminate in a temporal sequence that corresponds to their migratory route and cell fate, with NCCs that form the SG exiting the neural tube prior to those that form the DRG (Lallier and Bronner-Fraser, 1988; Le Douarin and Kalcheim, 1999; Tosney, 1978; Weston, 1970; George et al., 2007; Loring and Erickson, 1987; Thiery et al., 1982; Teillet et al., 1987; Erickson, 1985). The earliest, SG-fated NCCs

migrate ventrally either between the somites or between the neural tube and somite and differentiate directly into neurons, while later SG-destined NCCs migrate along the ventral border of the dermomyotome and through the sclerotome to form a perimeter composed of mitotically-active progenitor cells (Kasemeier-Kulesa et al., 2010). This change in migration pathway is likely mediated by SEMA3A and NRP1, since an increase in NCC migration through the intersomitic furrow is observed when the expression of either of these genes is ablated in the somite (Schwarz et al., 2009). All NCCs destined for the DRG associate with the sclerotome (Loring and Erickson, 1987; Teillet et al., 1987; Bronner-Fraser, 1986), with the last NCCs to colonize the ganglion also forming a perimeter of mitotically active progenitors (George et al., 2007, 2010). An interesting spatial dynamic of trunk NCC migration is the fact that although NCCs delaminate along the entire length of the neural tube, they migrate rostrally and/or caudally within the migration staging area (MSA) (Weston, 1991) to preferentially penetrate the anterior halves of each somite, in part due to repulsive EphrinB and Sema3F cues expressed in the posterior somite half (Gammill et al., 2006; Krull et al., 1997). In addition to cell membrane mediated guidance cues, NCCs destined to colonize the SG selectively express CXCR4 and chemotax towards periaortic sources of SDF-1 (Kasemeier-Kulesa et al., 2010; Saito et al., 2012).

Most studies of NCC migration have relied on static analyses to discern intercellular interactions. However, live time-lapse imaging of intact embryos and explants has revealed novel NCC behaviors (George et al., 2007, 2010; Krull et al., 1997; Clay and Halloran, 2010; Clay and Halloran, 2011; Jesuthasan, 1996; Kasemeier-Kulesa et al., 2006, 2005; Krull et al., 1995; Kulesa and Fraser, 1998; Kulesa et al., 2009, 2013, 2008; Langenberg et al., 2008; Teddy and Kulesa, 2004; Young et al., 2004; Druckenbrod and Epstein, 2005; Druckenbrod and Epstein, 2007). These studies have shown that NCCs are highly dynamic as they migrate, extending and retracting filopodia and moving in all four directions (dorsal, ventral, rostral, and caudal) as they interact with cues in their environment. Most NCC studies also tend to be "neural crest-centric", that is they do not describe the surrounding non-neural crest cell types with which NCCs interact along their migratory routes. Other than the clear effect the anterior versus posterior somite plays in patterning NCC migration (Schwarz et al., 2009; Gammill et al., 2006; Kalcheim and Goldstein, 1991; Newgreen et al., 1990), the potential influence of other non-NCCs on NCC behavior has not received much attention. In the trunk, a major cell type migrating at the same time and place as NCCs, are ECs as they form the embryonic vasculature. Static analyses in the trunk have demonstrated the colocalization of NCCs and ECs in the intersomitic furrow, around the dorsal aorta and postcardinal veins, and along the longitudinal anastomosis of the neural tube (Erickson, 1985; Schwarz et al., 2009; Miller et al., 2010; Spence and Poole, 1994). In the developing enteric nervous system (ENS), while one study did report a dependency of NCC migration in the hindgut along blood vessels (Nagy et al., 2009), other studies in both chick and mouse have found that the vascular and ENS systems develop autonomously or do not spatially align (Young et al., 2004; Delalande et al., 2014; Coventry et al., 1994; Landman et al., 2011). A study in zebrafish found no affect on DRG positioning in the absence of normal vascular patterning (Miller et al., 2010).

An emerging focus in both neurodevelopment and neurodegenerative disease is the "neurovascular link": that is, the recognition of extensive intercellular signaling between blood vessels, in particular, ECs and neurons, axons, and glia (Bautch and James, 2009; Carmeliet, 2003; Eichmann and Thomas, 2013; Gelfand et al., 2009; Bates et al., 2002; Taylor et al., 1994; Quaegebeur et al., 2011). The close congruency of blood vessel and peripheral nerve growth is well documented (Bates et al., 2002; Taylor et al., 1994; Vesalius, 1543), and numerous studies have shown that the developing vascular and peripheral nervous systems share guidance cues (Erskine et al., 2011; Suchting et al., 2005; Zacchigna et al., 2008). For example, blood vessels often track alongside peripheral nerves, while signals from both blood vessels and nerves can promote the branching and survival of each other (Burnstock and Ralevic, 1994; Martin and Lewis, 1989; Mukouyama et al., 2002). In the developing central nervous system (CNS), blood vessels have been shown to act as a substrate for migrating neuroblasts and olfactory bulb interneurons (Bovetti et al., 2007; Saghatelyan, 2009; Snapyan et al., 2009). In addition, the development, maintenance and proper functioning of both the nervous and vascular systems have been shown to be mutually interdependent via the secretion of growth factors including NGF, BDNF and VEGF (Schwarz et al., 2009; Eichmann and Thomas, 2013; Goldman and Chen, 2011; Haigh et al., 2004; Makita et al., 2008; Mukouyama et al., 2005; Sondell et al., 1999; Vieira et al., 2007; Zacchigna et al., 2008; Hashimoto et al., 2006). Neurons and endothelial cells share additional molecular pathways including Ephrins/Ephs; Nrpns/Semas/Plexins, Netrins, Notch/Delta, Slit/Robo, and SDF-1/CXCR4 (Kasemeier-Kulesa et al., 2010; Bouvree et al., 2008; Fujita et al., 2011; Gu et al., 2005; Herzog et al., 2001; Le Bras et al., 2006; Pan et al., 2007; Suchting et al., 2007; Weinstein, 2005). In the CNS, these bidirectional interactions are such that they comprise a "neurovascular unit" that includes neurons, glia, pericytes, and ECs, and this ensemble provides a critical stem cell niche in which mitotically active neural progenitors are found in close proximity to blood vessels (Bautch and James, 2009; Shen et al., 2004). Crosstalk between the two systems promotes the survival and maintenance of neurons and ECs and in fact, the neural degeneration that is the hallmark of many neurological diseases (e.g. Alzheimer's, Amyotrophic Lateral Sclerosis) is postulated to result from disruptions in this crosstalk (Zacchigna et al., 2008).

Given the significance of neurovascular interactions in other regions of the developing nervous system, we sought to investigate a potential "neurovascular link" during the formation of the trunk peripheral nervous system. To capitalize on the enhanced perspective provided by live imaging techniques, we used a line of transgenic quail, Tg(tie1:H2B-eYFP), in which endothelial cells are genetically engineered to express nuclear-localized enhanced yellow fluorescent protein (H2B-eYFP) (Sato et al., 2010). By simultaneously imaging NCCs tagged with monomeric cherry fluorescent protein (ChFP), and eYFP$^+$ ECs, we recorded these two distinct cells types interacting with each other in real time during the formation and patterning of the PNS. Our work reveals the extensive nature of these interactions and provides evidence for interconnectedness and interdependence between the nervous and vascular systems as they develop concurrently within the embryo.

2. Materials and methods

2.1. Quail embryos

The generation of a tie1 transgenic quail line Tg(tie1:H2B-eYFP) has been previously described (Sato et al., 2010) as well as our methods for electroporation of avian embryos (George et al., 2010). Briefly, for fluorescent labeling of NCCs, Japanese quail, (Coturnix coturnix japonica) embryos were incubated until Hamburger and Hamilton Stage (St.) 10–11 (Hamburger and Hamilton, 1992), and the fluorophore expressing plasmid, plenti-PGK:mCherry (Shaner et al., 2004), was injected at a concentration of 0.25 µg/µl in PBS until the entire length of the neural tube was filled. Electroporator settings were 5 pulses and 23 V with an interval of 100 ms.
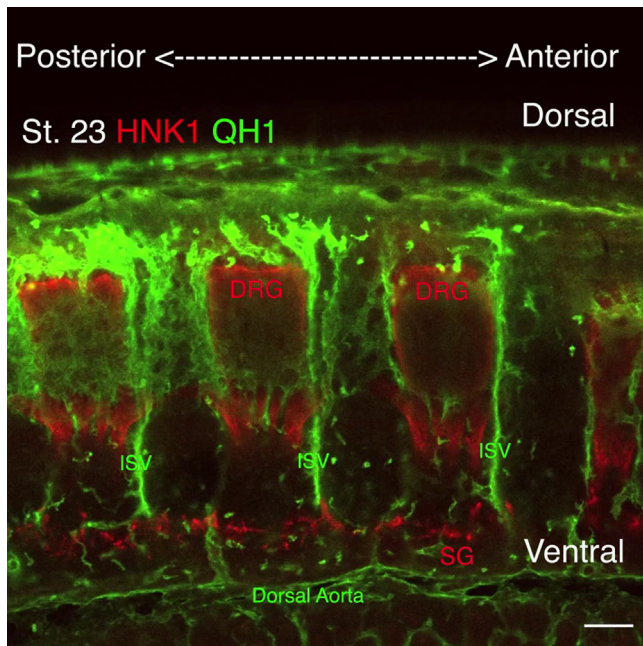
Movie 1A. By the end of NCC migration the peripheral ganglia and spinal nerves are surrounded by a vascular network. St. 23 quail. Fly thru Movie 1A shows a medial to lateral progression through the mid-trunk (between the wing bud and hind limb), beginning at the midsagittal plane that includes the embryonic spinal cord. The embryo was immunostained using primary antibodies that recognize NCCs and NCC derivatives (HNK1), and ECs and EC derived vasculature (QH1), cleared, and then cut in half along the sagittal midline (see methods). DRG, dorsal root ganglia; ISV, intersomitic vessel; PNVP, perineural vascular plexus; PSV, perisomitic vessel; SG, sympathetic ganglia. (Scale bar: 110 μm). Supplementary material related to this article can be found online at http://dx.doi.org/10.1016/j.ydbio.2016.02.028.

2.2. Immunohistochemistry (IHC)

Detailed methods for performing IHC using 16 μm cryosections, including embryo preparation, sectioning, and immunostaining, have been previously described (George et al., 2010). Unless otherwise stated, all IHC images correspond to the mid-trunk axial level. Mouse monoclonal primary antibodies anti-HNK1(IgM) (1:25) and anti-neurogenin2 (NGN2) (1:30,000) were gifts from Dr. Ben Novitch, UCLA. Anti-TUJ1 monoclonal mouse antibody (1:1000) was obtained from Covance (MMS-435P). Mouse monoclonal antibodies anti-PAX3, anti-Laminin, and anti-QH1 were obtained from the Developmental Studies Hybridoma Bank (http://dshb.biology.uiowa.edu) and used at a final concentration of 1 μg/ml. Rabbit polyclonal antibody anti-phospho-histone H3 (pH3) was obtained from Millipore (06-570).

For whole mount IHC, embryos were fixed in 4% PFA/PBS for 4–6 h (depending on age), and rinsed in PBS. For antibody staining, embryos were placed in scintillation vials and bathed in PBST (PBS and 0.5% triton X-100) for 40 min, followed by NGS block (20% normal goat serum, 1% glycine, 0.5% triton X-100 in 30 mM Tris, 150 mM NaCl) for 1 h, and incubated for 4 days with mouse monoclonal primary antibodies anti-HNK1 IgM (1 μg/ml) and anti-QH1 IgG (1 μg/ml) in NGS block. Embryos were then rinsed for 30 min in NGS block, rinsed for 5 h in PBST, and incubated for 1 h with NGS block prior to incubation in secondary antibodies [goat anti-mouse IgM, Alexa Fluor® 568 at 1:2000 (Thermo fisher scientific); goat anti-mouse IgG Fcγ 488 at 1:300 (Jackson Immuno research Labs)] in NGS block for 6 days. Embryos were then rinsed in PBST and stored overnight in PBS at 4 °C.
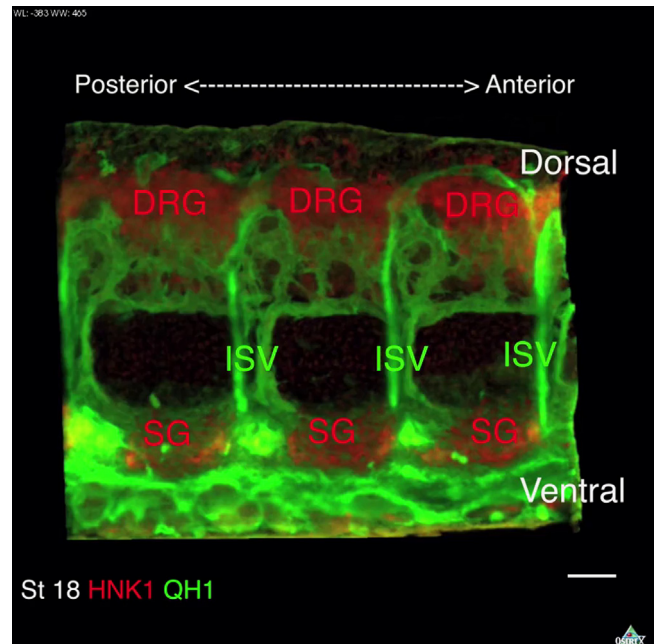
Movie 1B. The developing PNS and vasculature are tightly juxtaposed. St. 18 quail. Rotational Movie 1B shows a reconstructed view of the sagittal half of the mid-embryonic trunk. The embryo was immunostained with primary antibodies that recognize NCCs and NCC derivatives (HNK1), and ECs and EC-derived vasculature (QH1), cleared, and then cut in half along the sagittal midline (see methods). DRG, dorsal root ganglia; ISV, intersomitic vessel; PNVP, perineural vascular plexus; SG, sympathetic ganglia. (Scale bar: 120 μm). Supplementary material related to this article can be found online at http://dx.doi.org/10.1016/j.ydbio.2016.02.028.

2.3. Imaging

All static fluorescent images with the exception of Fig. 3A and B were captured using an inverted laser scanning confocal microscope (Olympus FV300) with 488 nm, 543 nm, and 633 nm laser lines and Fluoview Software v. 5.0. Objectives included a 20X Plan Apo (NA=0.70) dry objective and a 60X Plan Apo (NA=1.4) oil immersion lens (Olympus). Sections shown in 1B, 2B, 4C, 5A-F, and 6A, B, D were 16 μm.

For Movies 1A, 1B, the trunks of immunostained whole embryos were cut in half sagittally using a feather blade under a dissecting scope. For Movies 1A–1C, embryos were rendered optically transparent (cleared) prior to imaging using a methyl salicylate and benzyl benzoate (MSBB) method described previously (MacDonald and Rubel, 2008). Briefly, embryos were dehydrated using a series of ethanol solutions in distilled water (70%, 95%, 100%), and placed in a methyl salicylate, benzyl benzoate (5:3) solution for 30 min. All 3D images were acquired using the FV300 confocal and 20X objective described above, with a lateral (x-y) resolution of 0.69 μm per pixel and optically sectioned at 2 μm in Z. Confocal images were converted to 3D tiff-stacks using ImageJ (http://imagej.nih.gov/), and then imported to Osirix imaging software (http://www.osirix-viewer.com/) to generate rotational and fly thru movies (Movies 1A–1C).

For time-lapse imaging in Movies 2A and 2B, and photomicrographs shown in Figs. 2A and 3F and G, whole embryos were mounted on paper rings and transferred to Millicell-CM 0.4 mm culture plate inserts (Millipore, Bedford, MA) with the legs removed and saturated in neurobasal media (Invitrogen) supplemented with B27 (Invitrogen) within a 35 mm glass bottom dish (MatTek, Ashland, MA). Images of a single focal plane were captured every 5 min using the 20X dry objective on our FV300 (above) within an enclosure heated to 37 °C. For Movies 3E–3G, 4, 5, 6, and Fig. 3E, H–K, and 4B showing transverse slice
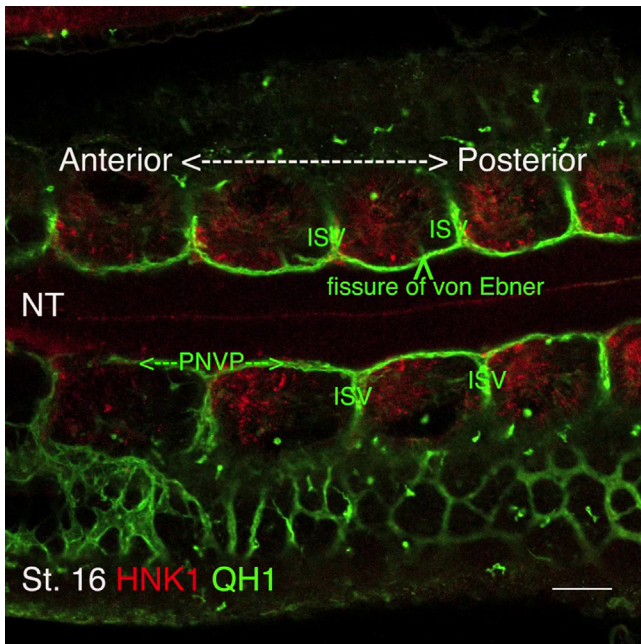
Movie 1C. NCCs are directly apposed to ECs as they enter the intersomitic furrow. St. 15/16 quail. Fly thru Movie 1C shows a dorsal to ventral progression through the dorsal half of the mid-embryonic trunk (somites 16–21). The embryo was immunostained using primary antibodies that recognize NCCs and NCC derivatives (HNK1), and ECs and EC-derived vasculature (QH1), cleared, and then imaged whole mount with the dorsal surface laid down on a cover glass. At this stage, the MSA is densely populated with NCCs with a few entering the intersomitic furrow in tight juxtaposition to ECs comprising the intersomitic vessel. The anterior half of the somite also shows some HNK1 immunoreactivity. DRG, dorsal root ganglia; ISV, intersomitic vessel; MSA, migration staging area; NCCs, neural crest cells; NT, neural tube. (Scale bar: 130 μm). Supplementary material related to this article can be found online at http://dx.doi.org/10.1016/j.ydbio.2016.02.028.

preparations, embryos were dissected in sterile, ice cold 1xPBS, embedded into low melting point agarose and sectioned at 250 μm using a vibratome. Transverse slices were then transferred to Millicell-CM 0.4 mm culture plate inserts (Millipore, Bedford, MA) saturated in neurobasal media (Invitrogen) supplemented with B27 (Invitrogen). The Millicell membrane with slice preparation was then cut from the plastic insert and placed in a 35 mm glass bottom dish (MatTek, Ashland, MA). Single focal plane images were captured every 5 min using the 20X objective on our FV300 within a heated enclosure.

For time-lapse imaging in Movies 2C and 3A–3D embryos were maintained ex ovo by mounting the specimens on paper rings as previously described (Cui et al., 2006; Rupp et al., 2008) and transferred to the environmentally controlled stage of a conventional microscope and wide-field time-lapse recordings were performed using an automated microscopy system; the instrumentation and methods have been described in detail elsewhere (Rupp et al., 2008; Czirok et al., 2002; Rupp et al., 2004, 2003). Twelve-bit gray-scale images were recorded every 7 min in both DIC and epi-fluorescence modes. Images were acquired at 7–9 focal planes, separated by 10 μm, and in most cases at multiple XY positions arranged as overlapping image tiles. This procedure over-sampled the specimen in X-Y-Z space thus ensuring that any point of interest remained in focus despite the normal movements of the embryo over the recording period (8–20 h). The imaging system was based on a computer-controlled standard compound Leica DMR inverted (Movies 2C) or upright (Movies 3A–3D) microscope equipped with a motorized stage and a QImaging Retiga-SRV TM camera, using a Leica 506057 N PLAN L 20X/0.40 CORR "Infinity Symbol"/0–2C objective (Movie 2C), or a Leica 556000 PL Fluotar 10X/0.25 P "Infinity symbol"/-objective (Movies 3A–3D).

Freely available, open source software code of our design (TiLa, KUMC) was used to process, align, smoothen and register the adjacent XY image tiles, from algorithm-selected Z planes, to produce a full-scale composite image for each time point (i.e., one movie frame). The resulting sequential image frames were concatenated and compiled as a movie file using ImageJ, then converted to MP4 format and annotated using Adobe Premiere Elements 14.

2.4. Quantification of EC density above the anterior versus posterior half somite

Time lapse recordings of St. 15 quail embryos obtained via the methods described above for Movies 3A–3D were used to quantify EC density. The fissure of von Ebner was used to delineate the anterior and posterior halves of somites 6–12, and the number of ECs present above each half was counted every 10 frames (or 70 min) over the course of 105 frames (or ∼12 h), $n=4$ embryos.

2.5. Quantification of proliferation

Data shown in Fig. 6C were obtained by counting the number of mitotically active (pH3$^+$) and non-mitotic (pH3$^-$) DRG progenitor cells (HNK1$^+$) within the DRG perimeter (outer-most cell layer only) that were in contact with ECs (QH1$^+$). DRG from 3 axial levels including the wing, trunk, and hind limb were included with no significant differences found between axial levels. For each DRG, the center section was determined, and the two sections flanking the center section were counted. For St. 26, 57 sections from 3 embryos were counted. For St. 22, 55 sections from 3 embryos were counted.

3. Results

At the level of the wing bud, NCCs begin delaminating from the neural tube at St. 13 and migrate ventrally both through the intersomitic furrow and between the neural tube and somite to form the SG (Lallier and Bronner-Fraser, 1988; Tosney, 1978; Erickson, 1985). The next cohort of delaminating NCCs (between St. 14–19) migrates ventrally to form the SG perimeter (Kasemeier-Kulesa et al., 2010), or stops next to the neural tube to form the DRG (Lallier and Bronner-Fraser, 1988). The third cohort to migrate ventrally (St. 17–20) does so either ipsilaterally or contralaterally to form the DRG perimeter (George et al., 2007), while the last cohort (St. 19–21) traverses laterally into the ectoderm to form melanocytes (Le Douarin and Kalcheim, 1999; Erickson et al., 1992; Rawles, 1948; Erickson and Goins, 1995).

3.1. Migrating neural crest cells and the nascent peripheral ganglia are tightly juxtaposed to the developing vasculature

To determine the position of migrating trunk NCCs and their derivatives relative to the developing vasculature, we fluorescently labeled both systems in fixed embryos at three developmental time points, collected images at successive focal planes throughout the trunk, and reconstructed these images three dimensionally. By St. 23, NCC migration is complete and the DRG and SG are composed of differentiating neurons and mitotically active neural progenitors (George et al., 2010). Movie 1A, a medial to lateral projection through the trunk of a St. 23 embryo, and Fig. 1A and B show a striking spatial apposition of the nascent sensory and sympathetic ganglia with the developing vasculature. NCC derivatives in the rostral most region of each DRG anlage are tightly apposed to ECs in the intersomitic vessel (ISV), while cells in the caudal region of each DRG anlage are in contact with ECs within

2A
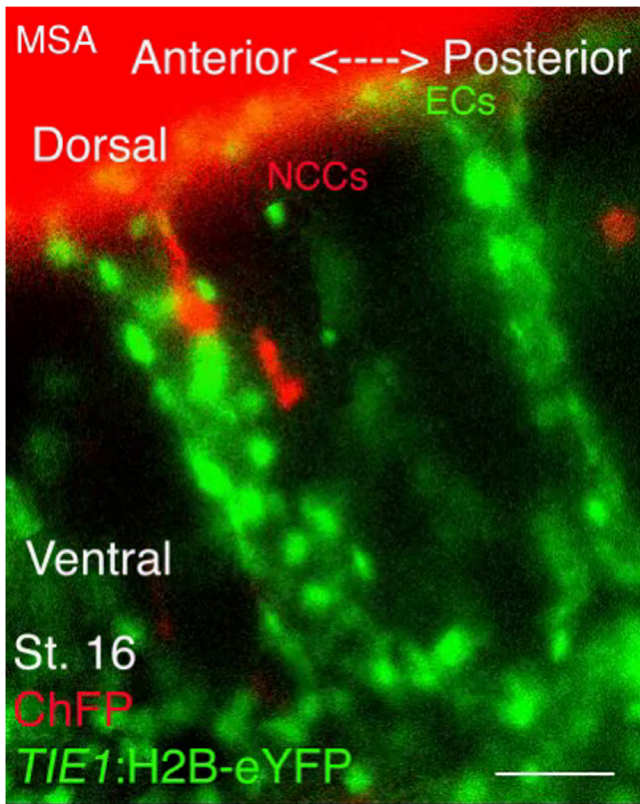
2B
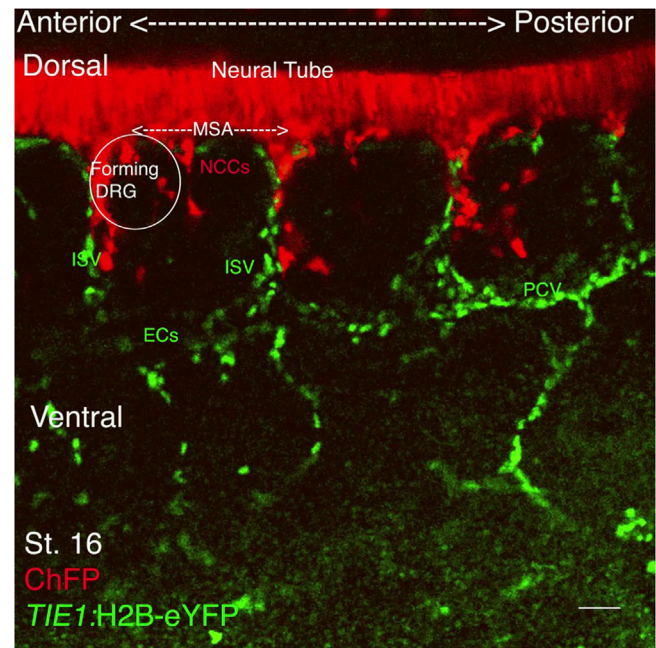
Movie 2. NCCs interact extensively with ECs as they migrate ventrally through the intersomitic furrow. Multispectral time-lapse confocal microscopy of a live, whole mount St. 16 Tg (*tie1*:H2B-eYFP) quail embryo viewed from the dorsolateral aspect. Axial level corresponds to the mid-trunk. The neural tube was electroporated with a ChFP expression plasmid at St. 11/12 to label the premigratory crest. NCCs track along the posterior surface of ECs as they migrate ventrally within the intersomitic furrow, making numerous filopodial contacts with ECs during their ventral migration. 2A zooms in on a single somite, while 2B shows more than three somites. 2A time-lapse duration = 15 h, 24 min. 2B time-lapse duration = 3 h, 20 min. DRG, dorsal root ganglia; ECs, endothelial cells; ISV, intersomitic vessel; MSA, migration staging area; NCCs, neural crest cells; PCV, postcardinal vein. (Scale bar: 2A, 45 μm; 2B, 36 μm). Supplementary material related to this article can be found online at http://dx.doi.org/10.1016/j.ydbio.2016.02.028.
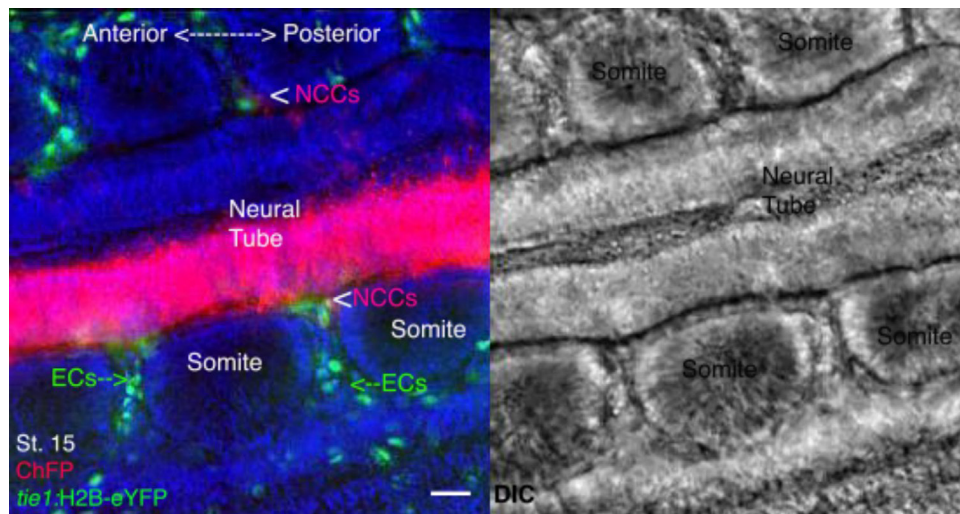

Movie 2C. NCCs make extensive contact with both ECs and the anterior face of the somite. St. 14–15 whole mount Tg (*tie1*:H2B-eYFP) quail embryos viewed from the dorsal aspect, somites 13–15. The neural tube was electroporated with a ChFP expression plasmid at St. 11/12 to label NCCs. In the left panel fluorescent time-lapse images are overlaid with DIC, allowing for visualization of the somite as well as migrating NCCs and ECs. NCCs enter the intersomitic furrow between the developing ISV and the anterior face of the somite, making extensive contact with both. The right panel shows DIC alone in grayscale to provide an enhanced perspective of the somites and the size of the intersomitic furrow. Time-lapse duration = 7 h, 44 min. ECs, endothelial cells; NCCs, neural crest cells. (Scale = 0.32 μm per pixel). Supplementary material related to this article can be found online at http://dx.doi.org/10.1016/j.ydbio.2016.02.028.

the fissure of von Ebner that forms at the anterior/posterior midpoint of the somite (Ebner, 1888). In fact, as shown in Fig. 1A and B, the anlagen appear completely circumscribed by ECs and a network of blood vessels that by now also surrounds each
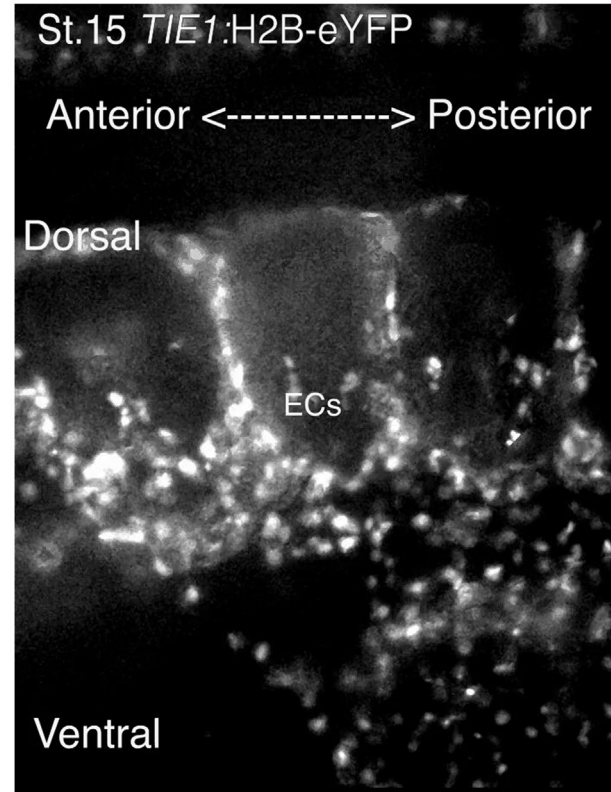
developing peripheral nerve. In particular, these reconstructions identify several potential NCC behaviors, including their migration and consolidation, that could be influenced by ECs.

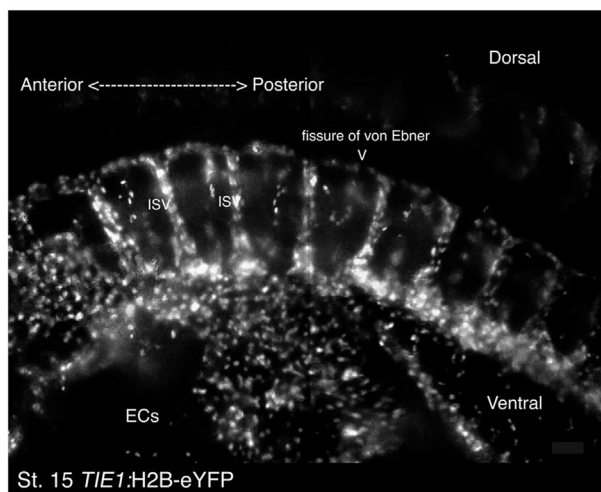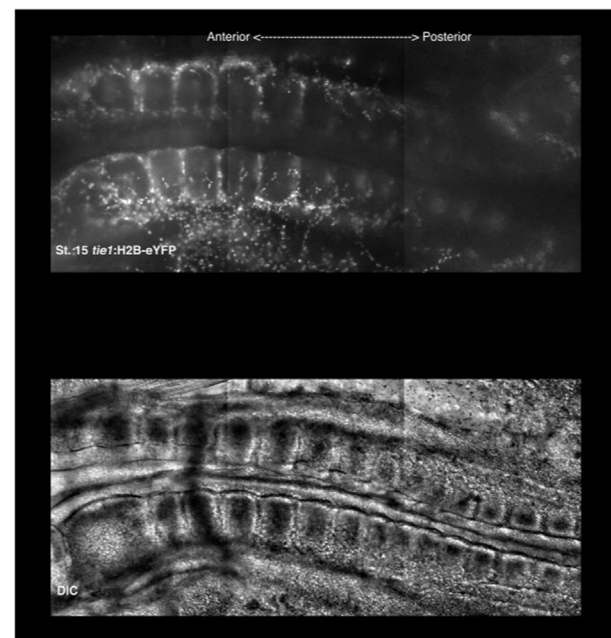We have previously documented the active segregation of NCCs

3A
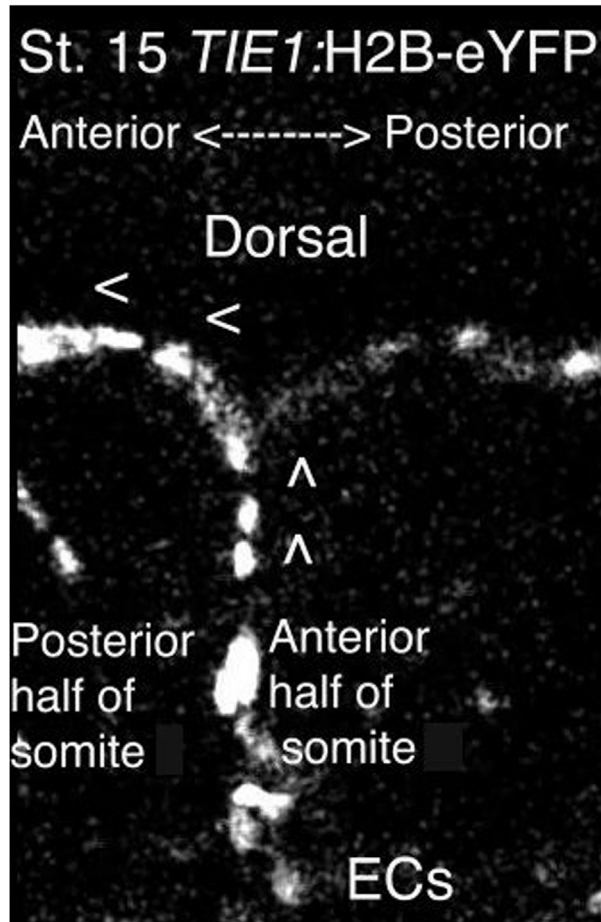
3B

3C

3D

Movie 3. EC migration patterns demarcate NCC boundaries. St. 15 whole mount Tg (tie1:H2B-eYFP) quail embryos viewed from the dorso-lateral aspect. Time-lapse imaging shows that ECs migrate in stereotyped patterns as they form the embryonic vasculature. ECs migrate dorsally within the intersomitic furrow until they reach the migratory staging area where they primarily turn in the anterior direction such that they asymmetrically cover the posterior half of the somite. Movie 3A zooms in on somites 4 and 5 and shows ECs migrating within a single intersomitic furrow. Movie 3B shows somites 3, 4 and 5 as well as 3 intersomitic furrows, and Movie 3C shows somites 3-11 and 9 intersomitic furrows. Movie 3D shows somites 3-16 with DIC in the lower panel. 3A time-lapse duration=3 h, 39 min. 3B,C time-lapse duration=16 h, 4 min. 3D time-lapse duration=13 h, 59 min. ECs, endothelial cells; ISV, intersomitic vessel. (Scale=0.64 μm per pixel). Supplementary material related to this article can be found online at http://dx.doi.org/10.1016/j.ydbio.2016.02.028.

as they form the sympathetic ganglia chain and that this process is dependent on EphB2/EphrinB1 interactions (Kasemeier-Kulesa et al., 2006). Movie 1B and Fig. 1C of a St. 18 embryo demonstrates

that the interganglionic area that we previously showed expresses EphrinB1, is in fact replete with a high density of ECs (arrows in Fig. 1C). Given that ECs are known to express EphrinB1 (Krull et al.,
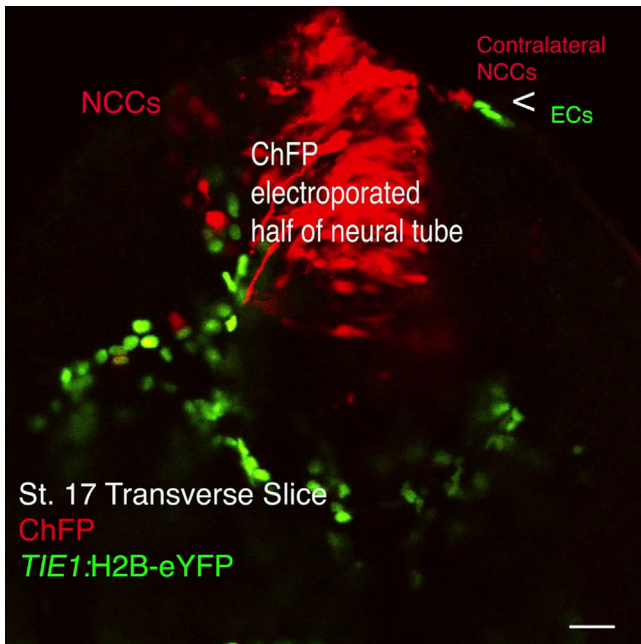
Movie 3E. EC patterning may help prevent NCCs from entering the posterior somite. Time-lapse confocal microscopy of a live, 200-μm transverse slice explant through the posterior half of a somite from the mid-trunk of a St. 17 Tg (*tie1*:H2B-eYFP) quail embryo shows contralaterally migrating NCCs within the MSA bumping up against ECs that appear to block them from further ventral migration. Time-lapse duration=6 h, 35 min. ECs, endothelial cells; NCCs, neural crest cells. (Scale bar: 24 μm). Supplementary material related to this article can be found online at http://dx.doi.org/10.1016/j.ydbio.2016.02.028.

1997), this raises the possibility that ECs are the source of EphrinB1 that drives the segregation of putative SG cells in the interganglionic region.

Movie 1C, a dorsal to ventral progression through the trunk of a St. 15 quail embryo, shows that the MSA where NCCs pause and accumulate subsequent to undergoing EMT but prior to ventral migration, positions NCCs directly dorsal to and juxtaposed to the developing vertebral blood vessels (Spence and Poole, 1994). Movie 1C and Fig. 1D also show that NCCs are tightly apposed to ECs that comprise the ISV as they enter the intersomitic furrow to migrate ventrally between the ISV and the anterior face of the somite

3.2. Early neural crest cells migrating within the intersomitic furrow interact extensively with endothelial cells and the anterior face of the somite

Having established the close physical proximity of ECs and NCCs in static reconstructions, we next sought to dynamically investigate the locations, migration patterns and behaviors of NCCs and ECs, relative to the somites, during the emergence of the trunk peripheral nervous system, specifically during development of the dorsal root and sympathetic ganglia.

The intersomitic vessels form by branching off of the dorsal aorta and postcardinal vein (Coffin and Poole, 1988; Isogai et al., 2001). Given the spatiotemporal proximity of early migrating NCCs and ECs within the intersomitic furrow where the ISV will form, we first characterized the interactions of these two cell types using time-lapse confocal microscopy of eYFP⁺ ECs [Tg (*tie1*:H2B-eYFP)] (Sato et al., 2010; Poynter and Lansford, 2008) and ChFP⁺ NCCs in whole mount embryos between St. 15–17. These time-lapses
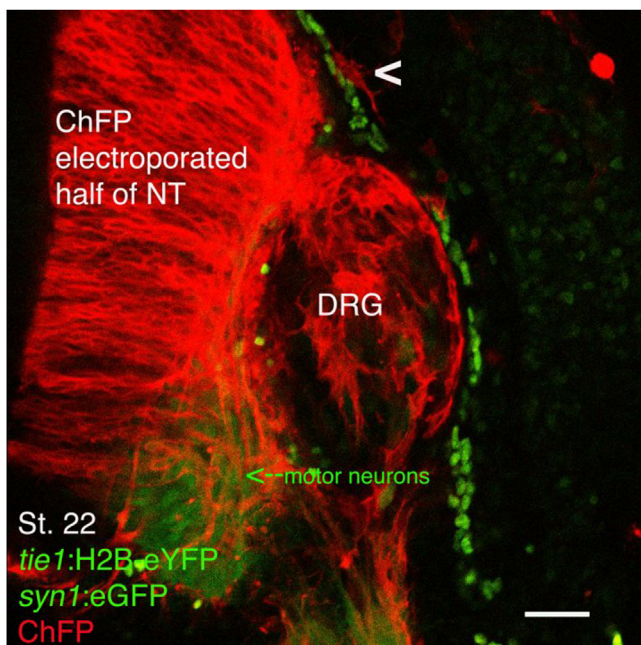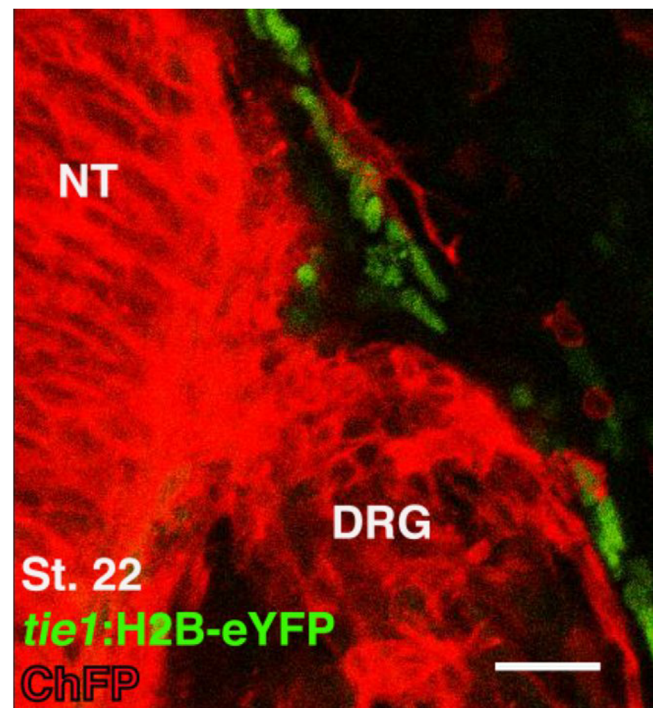
Movie 3F and G. A NCC changes its migration direction and morphology upon encountering a gap in the EC stream. St. 22 Tg (*tie1*:H2B-eYFP; *syn1*:eGFP) quail embryo in which the neural tube was electroporated with a ChFP expression plasmid at St. 11/12 to label the premigratory crest. In this transgenic line endothelial cells (*tie1*+) express nuclear localized eYFP, and differentiated neurons (*synapsin*+), including motor neurons and neurons in the core and ventral lateral region of the DRG, express cytoplasmic eGFP. Time-lapse confocal microscopy of a live, 200-μm transverse slice through the anterior somite shows the elongated morphology of a NCC (arrowhead) as it tracks in the ventrolateral direction along a relatively continuous layer of ECs, and how this morphology and trajectory change when the NCC encounters a gap in the vasculature. 3F,G time-lapse duration=4 h, 30 min. DRG, dorsal root ganglion. (Scale bar: 3F, 30 μm; 3G, 20 μm). Supplementary material related to this article can be found online at http://dx.doi.org/10.1016/j.ydbio.2016.02.028.
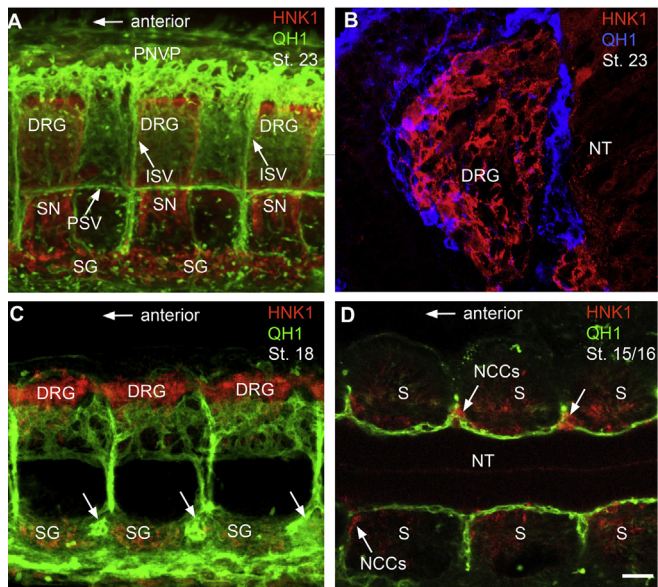
Fig. 1. The developing sensory and sympathetic ganglia are tightly juxtaposed to the developing vasculature. (A–D) Neural crest derivatives including the DRG and SG were labeled with HNK1 and the developing vasculature with QH1. (A, B) By St. 23 the DRG are completely surrounded by a vascular network. (A) Maximum intensity projection of the quail trunk viewed from the lateral aspect (for details see Movie 1A Legend). (B) 16 µm transverse cryosection. (C) Maximum intensity projection of the quail trunk viewed from the lateral aspect (for details see Movie 1B Legend). At St. 18, the developing dorsal root and sympathetic ganglia are tightly apposed to the developing vasculature and the interganglionic region between adjacent SG is densely populated with ECs (arrows). D) Frame 21 from Movie 1C of a St. 15/16 whole mount quail embryo. NCCs are tightly apposed to ECs as they enter the intersomitic furrow (arrows) to migrate ventrally between the ISV and the anterior face of the somite. The anterior somitic mesoderm also shows slight HNK1 immunoreactivity as previously documented in quail (Newgreen et al., 1990). DRG, dorsal root ganglia; ISV, intersomitic vessel; NCCs, neural crest cells; NT, neural tube; PNVP, perineural vascular plexus; PSV, perisomitic vessel; S, somite; SG, sympathetic ganglia; SN, spinal nerve. (Scale bar: A,C,D, 120 µm; B, 28 µm).
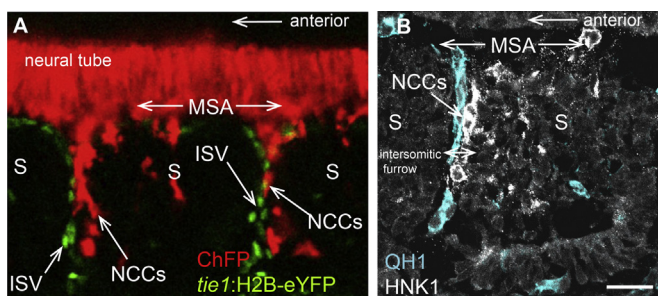
Fig. 2. Neural crest cells interact extensively with both endothelial cells and the somitic mesoderm during early neural crest cell migration. (A, B) St. 16 Tg(tie1:H2B-eYFP) quail. (A) Frame 1 from Movie 2B of a live, whole mount embryo viewed from the lateral aspect. Axial level corresponds to somites 14–16. Ventrally migrating NCCs appear to track along the developing ISV within the intersomitic furrow. NCCs were labeled with pLenti.PGK:mCherry (ChFP). (n=9 embryos). (B) 16 µm longitudinal cryosection of a St. 15 quail embryo, mid-trunk axial level. Membrane labeling of ECs using an anti-QH1 antibody and NCCs using an anti-HNK1 antibody. At this stage, the anterior half somite also shows slight HNK1 immunoreactivity (Newgreen et al., 1990). NCCs are tightly apposed to both ECs on their rostral side, and the anterior face of the somite on their caudal side. MSA, migration staging area; NCCs, neural crest cells; S, somite. (Scale bar: A, 50 µm; B,25 µm).

demonstrate that as NCCs move out of the MSA to migrate ventrally within the intersomitic furrow, they appear to migrate down and even track along the posterior side of the EC stream (Fig. 2A and Movies 2A and B). To visualize membrane-to-membrane contact between these two cell types and to determine whether

both cell populations move through the same longitudinal plane, we analyzed static longitudinal sections of quail embryos immunostained with QH1 antibody to visualize EC membranes, and HNK1 antibody to visualize NCC membranes. In these sections, early-migrating NCCs and ECs are tightly juxtaposed, making extensive intercellular contact within the intersomitic furrow (Fig. 2B). At these stages, the anterior half somite in quail embryos is somewhat HNK1 immunoreactive (Newgreen et al., 1990), allowing us to also visualize the proximity of NCCs to the anterior somite face. As shown in Fig. 2B, NCCs are tightly apposed to ECs on their rostral side, and to the anterior face of the somite on their caudal side. Movie 2C overlays fluorescent time-lapse images with differential interference contrast (DIC), allowing for visualization of the somitic environment, as well as migrating NCCs and ECs. The DIC channel is also shown in grayscale to provide an enhanced perspective of the somites and the size of the intersomitic furrow. These time-lapses and static images demonstrate that NCCs make extensive contact with both ECs and somitic mesoderm as they enter and migrate through the ISV.

3.3. Nascent vascular patterning demarcates neural crest migration boundaries

Our 3D reconstructions, live imaging, and analysis of static tissue sections demonstrate that early NCCs migrating between the somites move ventrally between rostrally adjacent ECs and the caudally adjacent anterior somite. NCCs were rarely observed on the anterior side of the EC stream or crossing the dorsal/ventral axis of the stream in the anterior direction (28 out of 844 migrating NCCs were observed on the anterior side of the developing ISV, $n=18$ embryos) (Fig. 2, Movies 2A and B). This behavior, where NCCS migrate along ECs rather than crossing through EC cell streams, suggests that EC patterning may influence NCC positioning and ventral migration, and thereby contribute to the anterior/posterior patterning of the PNS.

To investigate whether ECs might direct NCCs to enter the intersomitic furrow alongside the anterior versus the posterior somite face, we analyzed numerous time-lapse reconstructions of migrating ECs and quantified their positions in static tissue sections. Figs. 2, 3A, B and Movies 2A and B, 3A–3D show ECs migrating dorsally in a stream within the intersomitic furrow until they reach the MSA. Although ECs turn in both anterior and posterior directions once they reach the MSA, the majority turns anteriorly such that they extend over the posterior half of the anteriorly adjacent somite (Fig. 3A and B and Movies 3A–3D). Upon reaching the anterior/posterior midpoint of the somite, these ECs frequently turn ventrally again, exiting the MSA and diving into the somitic mesoderm where the fissure of von Ebner will emerge (Fig. 3B, arrows; Movie 3C), and contribute to the perineural vascular plexus (PNVP) (Wilting et al., 1995). This migration pattern, wherein the bulk of ECs turn anteriorly within the MSA and then exit the MSA before extending over the anterior half somite, results in an asymmetric distribution of ECs, with the majority dorsal to the posterior-half somite. To validate this observation, the numbers of ECs bordering the anterior versus the posterior halves of each somite were quantified in whole embryos. As shown in Fig. 3C, there are almost twice the number of ECs bordering the posterior half of the somite as compared to the anterior half ($n=4$ embryos). The schematic shown in Fig. 3D diagrams this basic migration pattern, also illustrated in time-lapse Movies 3B–3D.

The EC migration pattern shown in Fig. 3D likely generates a relatively continuous substratum positioned dorsally to the posterior half somite and extending ventrally into the intersomitic furrow (Fig. 3A, solid arrow). We posited that this "wall" of ECs covering the posterior half somite might block NCCs from
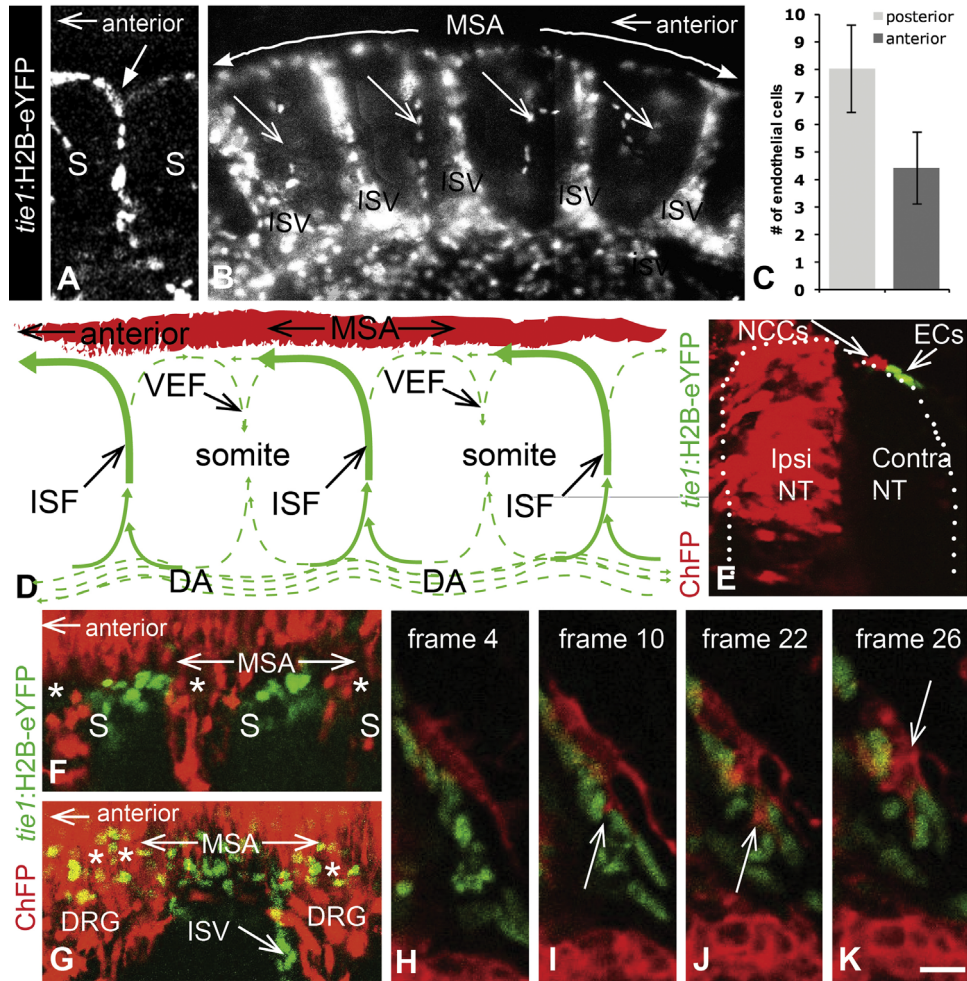
Fig. 3. Endothelial cell distribution may influence NCC migration and contribute to the rostral/caudal patterning of the peripheral nervous system. (A–D) St.15. Dorsally migrating ECs Tg (tie1:H2B-eYFP) primarily turn in the anterior direction when they reach the MSA, extending over the posterior half somite, and then exit the MSA before reaching the anterior half.(A, B) Individual frames from Movies 3A and 3C, respectively, showing a live, whole mount embryo viewed from the dorsolateral aspect. (A) Somites 4, 5. (B) Somites 3–8. (C) Quantification of the number of ECs located dorsal to the posterior versus the anterior half somite. Bars are standard deviation. $P < 0.0001$. (D) Schematic showing the basic migration pattern of ECs. (E–G) Axial level corresponds to the mid-trunk. (E) St. 17. In transverse explants through the posterior half somite, ECs are consistently located on the ventral side of NCCs and appear to block their ventral migration. To aid in the visualization of NCCs, a slice was chosen that includes contralaterally migrating NCCs. (F, G) Whole mount embryos viewed from the lateral aspect. (F) At St. 17, ECs are densely populated above the posterior half somite, and sparse above the anterior half (asterisks). (G) In contrast, by St. 20–22, ECs are more uniformly distributed along the length of the MSA although some gaps persist (asterisks). (H–K) St. 22. Individual frames from Movie 3G. (H) A NCC exhibits an elongated morphology as it migrates down a continuous layer of ECs. (I-K) The same NCC extends filopodia into a gap between adjacent ECs (arrows in I, J), followed by realignment of the cell such that the NCC soma moves into the same gap (arrow in K). Contra, contralateral; DA, dorsal aorta; ISF, intersomitic furrow; lpsi, ipsilateral; NCCs, neural crest cells; NT, neural tube S, somite; VEF, von Ebner's fissure. (Scale bar: A, 40 μm; B, 60 μm; E, F, G, 30 μm; H–K, 12 μm).

penetrating the posterior surface, and thereby facilitate their migration into the intersomitic furrow. In support of this hypothesis, ECs within the MSA at positions directly above (dorsal to) the posterior half somite were consistently located on the ventral side of NCCs (arrows in Fig. 3E). In addition, in both static images of longitudinal explants (Fig. 3F), and in time lapse imaging of transverse slice explants through the posterior somite (Movie 3E; arrowhead), ECs appear to form a barrier above the posterior somite half, potentially preventing NCC ventral migration. In contrast, the relative absence of ECs above the anterior half (asterisks in Fig. 3F), may facilitate NCC penetration into the anterior somite (Krull et al., 1997; Keynes and Stern, 1984).

Although ECs are more uniformly distributed along the length of the MSA towards the end of NCC migration (St. 20–22), there are still gaps between them such that late migrating NCCs can still access the ganglion (asterisks in Fig. 3G). Movies 3F and 3G and Fig. 3H–K show a live transverse slice through the anterior somite of a Stage 22 Tg(tie1:H2B-eYFP; syn1:eGFP) quail embryo including the developing DRG. In this transgenic line, endothelial cells

(tie1+) express nuclear-localized eYFP and differentiated neurons (synapsin+) express cytoplasmic eGFP including motor neurons and neurons in the DRG core and ventral lateral region (Seidl et al., 2013). Late NCCs are seen migrating ventrolaterally along ECs comprising the PNVP that surrounds the neural tube, which by now is somewhat continuous with the vasculature surrounding the DRG. These higher resolution images show the elongated morphology of a NCC as it migrates along a relatively continuous layer of ECs toward the DRG, and how this morphology changes when the NCC encounters a gap in the vasculature; it extends filopodia into the gap followed by a complete change in cell shape and alignment such that the cell body also begins squeezing through the gap toward the DRG. These time-lapse data strongly suggest that EC cell patterning influences NCC migratory behavior.

3.4. Neural crest cells track along the intersomitic vessel to colonize the sympathetic ganglia

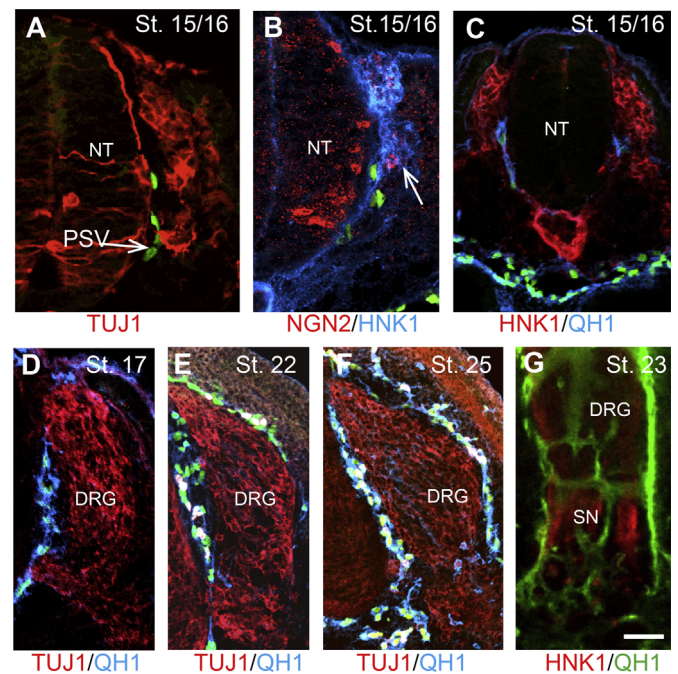Early NCCs that migrate ventrally within the intersomitic
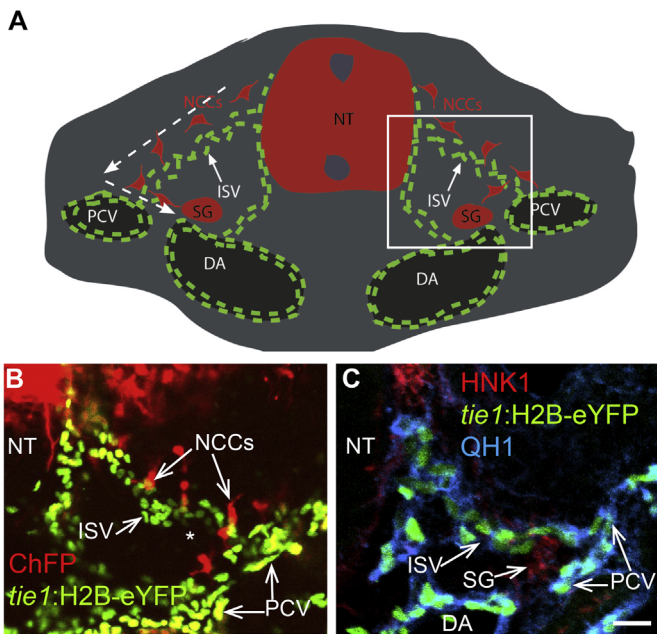
Fig. 4. Neural crest cells track along the developing intersomitic vessel to colonize the sympathetic ganglia. (A) Schematic of a transverse section through the trunk of a St. 17 quail embryo. The dashed line with arrowheads depicts the migration pattern of NCCs. The white box indicates the anatomical region shown in B and C. (B) Frame 4 from Movie 4 of a live transverse explant showing NCCs tracking along the intersomitic vessel until they reach the postcardinal vein, where they turn and migrate medially to colonize the sympathetic ganglia. (C) 16 μm transverse cryosection immunostained with anti-HNK1 to illustrate the position of the SG, as well as anti-QH1 to visualize EC membranes. DA, dorsal aorta; ISV, intersomitic vessel; NCCs, neural crest cells; NT, neural tube; PCV, postcardinal vein; SG, sympathetic ganglia. (Scale bar: B, 36 μm; C, 22 μm).


Fig. 5. Endothelial cells associate with early neural crest cells that seed the dorsal root ganglion and gradually encapsulate the ganglion as it condenses. (A–F) 16 μm transverse cryosections. Green nuclei correspond to ECs Tg(tie1:H2B-eYFP). (A) ECs that will form the perisomitic vessel are positioned at the motor axon exit point of the spinal cord and (B) likely contact NGN2+NCCs that "seed" the DRG. (C–F) As DRG development continues, ECs gradually circumscribe the entire ganglion. (G) Frame 45 from Movie 1A. ECs and the developing vasculature also encase the emerging spinal nerves. DRG, dorsal root ganglion; NT, neural tube; PSV, perisomitic vessel; SN, spinal nerve. (Scale bar: A, B 30 μm; C, 40 μm; D, E, F, G, 60 μm).

furrow are destined to colonize the sympathetic ganglia (Loring and Erickson, 1987; Thiery and Duband, 1982; Teillet et al., 1987; Erickson, 1985). The schematic in Fig. 4A shows the developing intersomitic vessel projecting both ventrally and laterally to the dorsal/ventral and medial/lateral level of the presumptive SG where it intersects the wall of the postcardinal vein (PCV) (Spence and Poole, 1994). Movie 4 of a live transverse explant, and Fig. 4B show that early-migrating NCCs continue to track along the ISV even at dorsal/ventral levels that position them beyond the ventral border of the somite. Similar to their behavior within the furrow, they move in a step-like fashion along the stream of ECs ventrolaterally toward their target next to the dorsal aorta. These NCCs remain on the lateral side of the ISV, and do not cross the EC stream, until they encounter a second, larger stream of ECs running in the anterior/posterior direction that form the wall of the PCV. After contacting the PCV, NCCs turn and migrate through the intersomitic stream to the presumptive location of the SG. The dashed line with arrowheads in Fig. 4A shows this basic migration pattern. Fig. 4C shows a similar transverse cryosection immunostained with HNK1 antibody to identify the location of the developing SG (compare HNK1 staining in Fig. 4C to NCC positioning in Fig. 4B and Movie 4). Movie 4 also shows how contact with a pioneer NCC already in the SG anlage may help recruit the more dorsal NCC to colonize the SG.

3.5. Neural crest contact with the perisomitic vessel may establish the ventral border of the DRG and induce the "back fill" colonization of the dorsal root ganglion

Using both Tg(tie1:H2B-eYFP) quail and immunostaining with the EC marker QH1, we observed a discrete population of ECs at St.12/13 that are consistently located at the motor axon exit point

from the spinal cord (Fig. 5A). These ECs are in the perisomitic vessel (PSV) (Schwarz et al., 2009), also referred to as the longitudinal anastomosis (Miller et al., 2010). Their stereotyped localization positions them for contact with the earliest migrating NCCs that travel between the neural tube and the somite (Loring and Erickson, 1987; Schwarz et al., 2009; Miller et al., 2010). The majority of this NCC cohort migrates to the sympathetic ganglia via an SDF-1/CXCR4 mediated chemotaxis, but a minority seed the future DRG (Kasemeier-Kulesa et al., 2010; George et al., 2010). Previous studies show that the first NCCs that colonize the DRG anlagen express the basic helix-loop-helix transcription factor Ngn2 (Ma et al., 1999) and act as a nucleation site around which later-migrating NCCs condense (George et al., 2010; Marmigere and Ernfors, 2007). We noticed that these Ngn2+NCCs are typically located at the ventromedial border of what will be the DRG and asked whether their cessation in migration at that point correlates spatially with the PSV. Analysis of static tissue sections shows that NCCs immediately adjacent to the neural tube are frequently Ngn2+, and based on their relative positions, likely contact PSV ECs (Fig. 5B,C). To investigate the dynamics between these two cell types we imaged their interaction in live tissue. Movie 5 shows how ventrally migrating NCCs begin to stack up dorsally on top of the PSV when they encounter the developing vessel. Fig. 1A and Movie 1B also show how the more mature PSV spatially aligns with the ventral border of the DRG.

3.6. Endothelial cells encapsulate the nascent dorsal root ganglion and the emerging spinal nerves

As DRG development continues, ECs gradually circumscribe the DRG and by St. 23–25 encapsulate the entire ganglion and the emerging spinal nerves (Fig. 5 D–G; Movie 1A). Although cell-to-
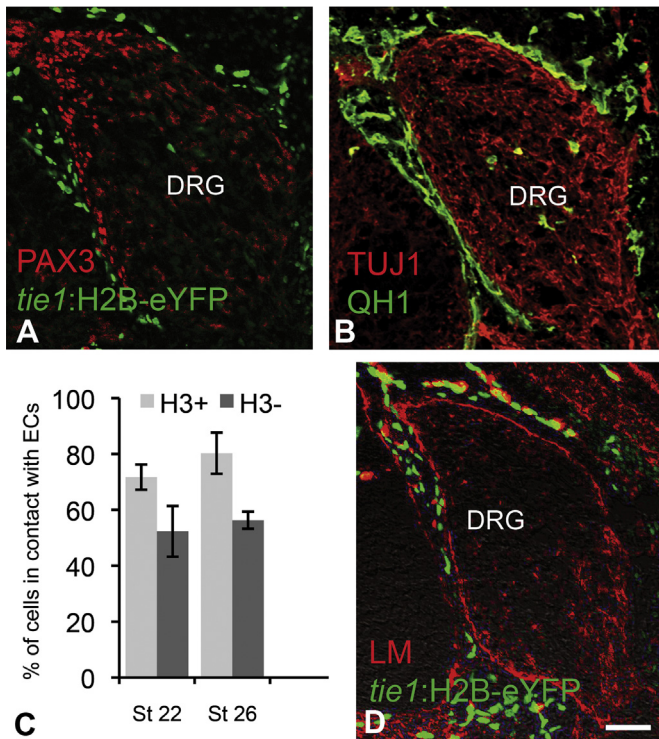
Fig. 6. Contact with endothelial cells may influence the mitotic activity of dorsal root ganglia progenitors. (A, B, D) St. 26/27, 16 μm transverse cryosections. (A, B) Adjacent serial sections show that PAX3+ progenitors within the dorsal pole of the DRG and along the medial perimeter and dorsolateral perimeter are geographically and temporally aligned with ECs. (C) Perimeter-localized DRG progenitors in M phase (H3+) are more likely to be in contact with ECs as compared to non-proliferating cells, with 80% of H3+ progenitors being in contact with ECs during the peak of proliferation at St. 26/27. Bars are standard error. $P=0.03$ for St. 22; $P=0.006$ for St. 26. (D) A layer of laminin (LM) resides between perimeter-localized DRG progenitor cells and apposed ECs. DRG, dorsal root ganglion. (Scale bar: A, B, D 36 μm).

cell cohesion likely functions in constraining NCCs to the condensing DRG, our time-lapse imaging reveals continual interactions between NCCs and these border ECs that also appear to constrain NCCs (Movie 6). NCCs that initiate movements out of the anlage often reverse this motion or retract their filopodia following contact with a border EC. Movie 1A and Fig. 5G also show how the emerging spinal nerves are tightly associated with a network of vasculature.

3.7. Proximity to endothelial cells is associated with mitotic activity of dorsal root ganglia progenitor cells

As the DRG matures, a fundamental segregation manifests in which differentiating neurons are confined to the inner core, while mitotically active progenitor cells colonize the perimeter (George et al., 2007, 2010; Rifkin et al., 2000). We have shown previously that the DRG perimeter is comprised of two molecularly distinct progenitor zones: cells within the dorsal pole and along the medial and dorsolateral perimeter express PAX3 and SOX10, while those along the ventrolateral perimeter are SOX10+/PAX3− (George et al., 2010). We have also shown that the PAX3+ subset goes on to specifically give rise to the majority of TRKA+ pain and temperature responsive sensory neurons, while the SOX10+ cells stay in the cell cycle and give rise to glial cells (George et al., 2010). Here we show an asymmetry in the pattern of EC condensation around the DRG perimeter that is spatially and temporally aligned with the PAX3+ zone, with numerous ECs tightly apposed to PAX3+ progenitors (Fig. 6A,B). In contrast, there are relatively few

ECs along the PAX3− zone that comprises the lateral and ventral perimeter of the DRG. Since sensory neurogenesis precedes gliogenesis (George et al., 2010; Carr and Simpson, 1978; Wakamatsu et al., 2000), we asked whether mitotically-active progenitors within the DRG perimeter were more likely to be in contact with ECs, than were non-proliferating cells within the perimeter. That analysis (Fig. 6C) reveals that in fact progenitors in M phase are more likely to be in contact with ECs as compared to non-proliferating progenitor cells. During the peak of proliferation (St. 26/27), an average of 80% of cycling pH3+ progenitors were in contact with ECs (n=3 embryos, 246 cells). Interestingly, at younger ages (St. 21/22), while cycling cells were still more likely to be in contact with ECs compared to non-cycling cells, the difference was less dramatic suggesting that other, non EC-associated mitogenic sources drive progenitor cell proliferation at earlier time points. During the peak period of PAX3+ progenitor cell proliferation, a dense layer of laminin (Fig. 6D) is deposited between the DRG progenitors and the apposed ECs. Since the extracellular matrix is a repository of growth factors and mitogens including fibroblast growth factors (FGFs), insulin-like growth factors (IGFs) hepatocyte growth factors (HGFs), transforming growth factors (TGFs), platelet-derived growth factors, and vascular endothelial growth factor (VEGF), it may act as a mediator of communication between these DRG progenitors and ECs (Taipale and Keski-Oja, 1997).

4. Discussion

This is the first study to image in real time the intercellular interactions between migrating neural crest cells and endothelial cells during development of the PNS. In this study, we have exploited the power of live imaging technologies in transgenic quail that express both neural and endothelial cell fluorescent markers to image neural crest cells migrating in their *in vivo* environment and interacting with neighboring cell types, in this case, endothelial cells. Similar to other live imaging studies that have revealed novel intercellular and molecular interactions not previously discerned from analyses of static tissue (Kasemeier-Kulesa et al., 2006, 2005; Kulesa et al., 2013; Lichtman and Fraser, 2001), this work reveals novel, hitherto undescribed dynamic intercellular interactions that implicate key functions for ECs during NCC migration and condensation as they form dorsal root and sympathetic ganglia *in vivo*. Our data demonstrate that NCCs interact with ECs at key junctures during their migration and differentiation including: 1) as NCCs migrate along the MSA; 2) as they enter and migrate through the intersomitic furrow; 3) as they segregate to form discrete sympathetic ganglia; 4) when the first NCCs that seed the DRG stop at the future ventral-most axis of the DRG anlage; 5) during formation of DRG boundaries; 6) as the developing spinal nerves become encased in vasculature; 7) during the proliferation of perimeter-localized DRG progenitor cells. With a new awareness of the interactive relationship between endothelial cells and neural crest cells, the goal will be to identify the molecular mechanisms that orchestrate and mediate these behaviors. In summary, the data presented here underscore the power of the Tg *tie1* quail as a novel and powerful tool for studying EC migration patterns and demonstrate that EC movements, in particular during formation of the intersomitic vessels and their asymmetric colonization above the anterior and posterior halves of the somite, are more complex than have been previously reported (Gore et al., 2012; Stainier et al., 1995).

Analysis of our live imaging data supports a model in which ECs both direct and constrain the migratory behavior and path of NCCs during development of the PNS. While it is conceivable that both NCCs and ECs could be responding to the same guidance cues in shared locations, the fact that NCCs alter their migratory route
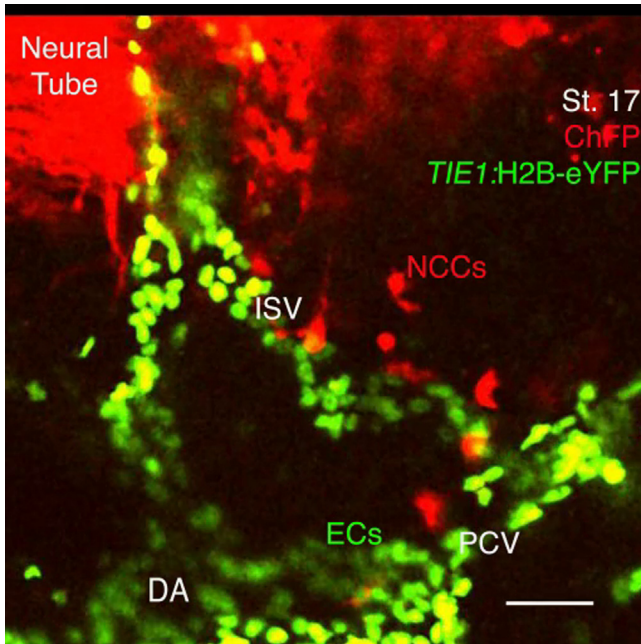
Movie 4. ECs appear to direct early migrating NCCs toward the sympathetic ganglia. St. 17 Tg (*tie1*:H2B-eYFP) quail in which the neural tube was electroporated with a ChFP expression plasmid to label NCCs. Time-lapse confocal microscopy of a live, 200-μm transverse slice explant. A developing intersomitic vessel is shown with NCCs tracking along ECs as they migrate ventrolaterally until they reach the PCV, where they turn and migrate medially to colonize the SG. Time-lapse duration=2 h, 25 min. DA, dorsal aorta; ECs, endothelial cell; ISV, intersomitic vessel; NCCs, neural crest cells; PCV, postcardinal vein; SG, sympathetic ganglia. (Scale bar: 40 μm). Supplementary material related to this article can be found online at http://dx.doi.org/10.1016/j.ydbio.2016.02.028.
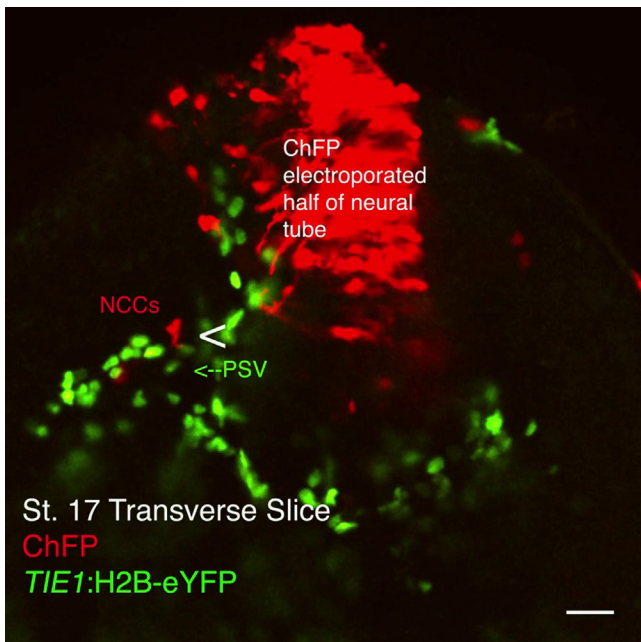
Movie 5. NCCs that encounter the perisomitic vessel stop their ventral migration and colonize the DRG. St. 17 Tg (*tie1*:H2B-eYFP) quail in which the neural tube was electroporated with a ChFP expression plasmid to label NCCs. Time-lapse confocal microscopy of a live, 200-μm transverse slice explant shows how NCCs that have migrated as far ventrally as the perisomitic vessel, appear to stop their ventral migration upon contact with the vessel, which thereby defines the ventral-most point of the DRG anlage. Time-lapse duration=6 h, 40 min. NCCs, neural crest cells; PSV, perisomitic vessel. (Scale bar: 24 μm). Supplementary material related to this article can be found online at http://dx.doi.org/10.1016/j.ydbio.2016.02.028.
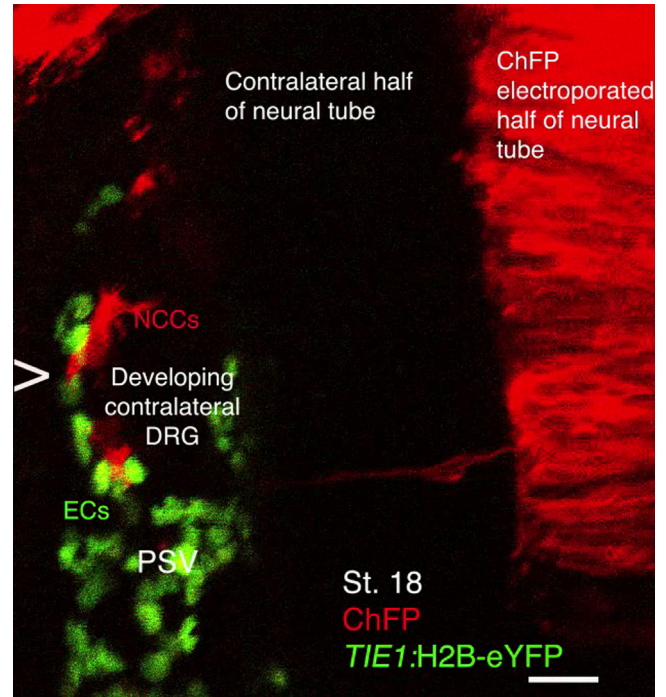
Movie 6. ECs may constrain NCCs and prevent their migration away from the DRG. Movie 6 shows the contralateral half of a 200 μm transverse slice explant from a St. 18 Tg (*tie1*:H2B-eYFP) quail in which the neural tube was electroporated with a ChFP expression plasmid to label NCCs. Since only contralaterally migrating NCCs are labeled on the non-electroporated half, viewing this side aids in the visualization of individual NCCs and filopodial dynamics. Time-lapse confocal microscopy shows how ECs begin to encapsulate the nascent DRG and appear to constrain NCCs within the condensing anlage. Time-lapse duration=4 h, 55 min. DRG, dorsal root ganglion; ECs, endothelial cells; NCCs, neural crest cells; PSV, perisomitic vessel. (Scale bar: 24 μm). Supplementary material related to this article can be found online at http://dx.doi.org/10.1016/j.ydbio.2016.02.028.

following direct contact with ECs suggests their behavior is influenced by this contact, rather than by some other environmental cue. Depending on the location, ECs provide either a permissive substrate facilitating NCC migration, or they appear to constrain movement, preventing the emigration of nascent DRG cells from the anlage and restraining further ventral migration into the developing SG. This last behavior was described in an previous study (Kasemeier-Kulesa et al., 2005) in which we showed that at early stages, NCCs in the DRG and SG anlagen could exchange locales, but by St. 17 a "boundary" was established that clearly inhibited NCCs from entering the more dorsal or ventral ganglia. Here we show that this boundary correlates temporally and spatially with the perisomitic vessel, or longitudinal anastomosis (Schwarz et al., 2009; Miller et al., 2010).

Prior observations of the close apposition of migrating NCCs and the ISVs have posited that they independently respond to shared cues in the intersomitic furrow (Erickson, 1985; Schwarz et al., 2009; Miller et al., 2010; Spence and Poole, 1994). One study demonstrated that DRG form in their normal locations in the zebrafish mutant, *cloche,* in which some blood vessels, including the ISVs are eliminated, suggesting that DRG formation is independent of these vessels (Miller et al., 2010; Stainier et al., 1995). However, the major anterior/posterior vessels form normally in *cloche* embryos, including the dorsal aorta, and numerous individual ECs in the location of the ISVs are still present (Miller et al., 2010). Moreover, since early NCCs that migrate within the intersomitic furrow colonize the SG rather than the DRG, we would predict that SG, rather than DRG, formation would be impacted by loss of the intersomitic vessels. The fibronectin rich extracellular matrix associated with the ISV likely promotes NCC

adhesion to ECs and migration along them, such that early NCCs migrate ventrally between the ISV and the somite (Spence and Poole, 1994), rather than penetrating the anterior half somite precociously. Multiple previous studies have shown a spatio-temporal correlation between the presence of fibronectin and NCC migration, as well as the cessation of NCC movement with the local disappearance of fibronectin. *In vitro* studies have also shown fibronectin and cultured ECs to be an excellent substrate for NCC adhesion and motility (Thiery and Duband, 1982; Spence and Poole, 1994; Thiery and Duband, 1986, 1985).

Ephrins are important signaling molecules mediating the development of both the neural crest and endothelial lineages (Gammill et al., 2006; Wang and Anderson, 1997). A previous study demonstrated that avian ECs that are positioned above (dorsal to) the posterior half somite and extending into the entrance to the intersomitic furrow express EphrinB2 (Krull et al., 1997). These are the same ECs that our live time-lapses document interacting with NCCs as they leave the MSA to enter the furrow and that appear to provide a substrate for NCCs as they migrate ventrally within the furrow (Movies 2A and 2B). Although early expression of ephrin ligands in the avian dermomyotome prevents NCCs from entering the dorsolateral pathway, later expression of EphrinB2 within the dermomyotome promotes the migration of late NCCs (melanoblasts) into this same pathway (Santiago and Erickson, 2002). Thus similar to the dual role that ephrins play in the dorsolateral pathway, ephrins may also play opposing roles in relation to the ventral pathway; although EphrinB1 expression within the avian posterior half-sclerotome blocks the ventral migration of NCCs (Krull et al., 1997), EphrinB2 expression by ECs may actually recruit NCCs out of the MSA and stimulate their procession into the intersomitic furrow. In support of this model, the binding of EphrinB2 ligands by NCC EphB receptors has been shown to promote NCC motility by increasing cell adhesion (Santiago and Erickson, 2002). Alternatively, since siRNA knock-down of EphrinB2 causes reduced filopodial activity in ISV endothelial tip cells, EphrinB2 could play a less direct role in promoting NCC migration via simply promoting EC/NCC contact (Gore et al., 2012). The ultimate test of a role for ECs in patterning NCC migration will require the elimination of ECs in a spatially, temporally and cell type-specific controlled manner, as any crude systematic elimination can induce indirect effects.

This study is not the first to report interactions between ECs and NCCs that influence PNS development. Recent *in vitro* studies demonstrate that co-culturing of ECs and vascular smooth muscle cells with human embryonic stem cell derived-NCCs induced their differentiation into sensory and autonomic neurons (Acevedo et al., 2015). Interestingly, many vascular smooth muscle cells are themselves derived from the neural crest (Beall and Rosenquist, 1990; Etchevers et al., 2001; Jiang et al., 2000; Li et al., 2013; Liang et al., 2014) pointing to the multiple nodes of interactions between these two lineages. Previous work in chick embryos has shown that dorsal aorta-derived BMPs are required for differentiation of sympathetic neurons (Saito et al., 2012; Reissmann et al., 1996) and in zebrafish it has been recently reported that PDGFR-mediated maturation of vascular mural cells is required for full differentiation of a sympathetic, noradrenergic fate (Fortuna et al., 2015). The cardiac crest is well known to be integrally involved in development of the cardiovascular system coordinating with ECs and smooth muscle cells to generate the outflow tract and cardiac cushions via SEMA3C and NRP1 (Plein et al., 2015). Similarly the cephalic crest also plays a key role in mediating the vascularization of the facial cartilage by producing a vital source of VEGF (Wiszniak et al., 2015) and ECs are essential for promoting the migration and survival of cranial neural crest cells (Milgrom-Hoffman et al., 2014). Thus the multistep differentiation process of these two embryologically distinct lineages are highly interdependent and converge spatially and temporally to regulate each other's development.

In the PNS, our understanding of how these two embryologically distinct systems first interact and the significance of their interactions as they form is sparse, nor do we understand the mechanisms that lead to peripheral neuropathy should this neurovascular cross talk break down. By live imaging the development of the vascular and peripheral nervous systems with cell type-specific markers, we present here the first evidence for direct interactions between these two systems in real time. Our studies demonstrate that ECs and NCCs interact extensively during formation of the sensory and sympathetic ganglia, and suggest that ECs provide critical guidance cues, either positive or negative depending on their location, to migrating NCCs. With further elucidation of the genes and pathways that mediate communication between NCCs and ECs, a more comprehensive understanding of the interdependency of these two systems both during development and disease will be possible.

References

Acevedo, L.M., Lindquist, J.N., Walsh, B.M., Sia, P., Cimadamore, F., Chen, C., Denzel, M., Pernia, C.D., Ranscht, B., Terskikh, A., Snyder, E.Y., Cheresh, D.A., 2015. HESC differentiation toward an autonomic neuronal cell fate depends on distinct cues from the co-patterning vasculature. Stem Cell. Rep. 4 (6), 1075–1088. http://dx.doi.org/10.1016/j.stemcr.2015.04.013, PubMed PMID: 26004631; PMCID: PMC4471822.

Bronner-Fraser, M., 1986. Analysis of the early stages of trunk neural crest migration in avian embryos using monoclonal antibody HNK-1. Dev. Biol. 115 (1), 44–55, PubMed PMID: 3516760.

Bautch, V.L., James, J.M., 2009. Neurovascular development: The beginning of a beautiful friendship. Cell Adhes. Migr. 3 (2), 199–204, PubMed PMID: 19363295; PMCID: PMC2679887.

Bates, D., Taylor, G.I., Newgreen, D.F., 2002. The pattern of neurovascular development in the forelimb of the quail embryo. Dev. Biol. 249 (2), 300–320, PubMed PMID: 12221008.

Burnstock, G., Ralevic, V., 1994. New insights into the local regulation of blood flow by perivascular nerves and endothelium. Br. J Plast. Surg. 47 (8), 527–543, PubMed PMID: 7697280.

Bovetti, S., Bovolin, P., Perroteau, I., Puche, A.C., 2007. Subventricular zone-derived neuroblast migration to the olfactory bulb is modulated by matrix remodelling. Eur. J Neurosci. 25 (7), 2021–2033. http://dx.doi.org/10.1111/j.1460-9568.2007.05441.x, PubMed PMID: 17439490.

Bouvree, K., Larrivee, B., Lv, X., Yuan, L., DeLafarge, B., Freitas, C., Mathivet, T., Breant, C., Tessier-Lavigne, M., Bikfalvi, A., Eichmann, A., Pardanaud, L., 2008. Netrin-1 inhibits sprouting angiogenesis in developing avian embryos. Dev. Biol. 318 (1), 172–183. http://dx.doi.org/10.1016/j.ydbio.2008.03.023, PubMed PMID: 18439993.

Beall, A.C., Rosenquist, T.H., 1990. Smooth muscle cells of neural crest origin form the aorticopulmonary septum in the avian embryo. Anat. Rec. 226 (3), 360–366. http://dx.doi.org/10.1002/ar.1092260313, PubMed PMID: 2327605.

Clay, M.R., Halloran, M.C., 2010. Control of neural crest cell behavior and migration: Insights from live imaging. Cell. Adhes. Migr. 4 (4), 586–594, Epub 2010/07/31. doi: 12902 [pii] 10.4161/cam.4.4.12902. PubMed PMID: 20671421; PMCID: 3011273.

Clay, M.R., Halloran, M.C., 2011. Regulation of cell adhesions and motility during initiation of neural crest migration. Curr. Opin. Neurobiol. 21 (1), 17–22, Epub 2010/10/26. doi: S0959-4388(10)00183-2 [pii] 10.1016/j.conb.2010.09.013. PubMed PMID: 20970990; PMCID: 3049825.

Coventry, S., Yost, C., Palmiter, R.D., Kapur, R.P., 1994. Migration of ganglion cell precursors in the ileoceca of normal and lethal spotted embryos, a murine model for Hirschsprung disease. Lab Investig. 71 (1), 82–93, PubMed PMID: 8041122.

Carmeliet, P., 2003. Blood vessels and nerves: common signals, pathways and diseases. Nat. Rev. Genet. 4 (9), 710–720. http://dx.doi.org/10.1038/nrg1158, PubMed PMID: 12951572.

Cui, C., Lansford, R., Filla, M.B., Little, C.D., Cheuvront, T.J., Rongish, B.J., 2006. Electroporation and EGFP labeling of gastrulating quail embryos. Dev. Dyn. 235 (10), 2802–2810. http://dx.doi.org/10.1002/dvdy.20895, PubMed PMID: 16894628.

Czirok, A., Rupp, P.A., Rongish, B.J., Little, C.D., 2002. Multi-field 3D scanning light microscopy of early embryogenesis. J Microsc. 206 (Pt 3), 209–217, PubMed PMID: 12067365.

Coffin, J.D., Poole, T.J., 1988. Embryonic vascular development: immunohistochemical identification of the origin and subsequent morphogenesis of the major vessel primordia in quail embryos. Development 102 (4), 735–748, PubMed PMID: 3048971.

Carr, V.M., Simpson Jr., S.B., 1978. Proliferative and degenerative events in the early development of chick dorsal root ganglia. II. Responses to altered peripheral fields. J Comp. Neurol. 182 (4), 741–755. http://dx.doi.org/10.1002/cne.901820411, PubMed PMID: 721976.

Druckenbrod, N.R., Epstein, M.L., 2005. The pattern of neural crest advance in the cecum and colon. Dev. Biol. 287 (1), 125–133. http://dx.doi.org/10.1016/j.ydbio.2005.08.040, PubMed PMID: 16197939.

Druckenbrod, N.R., Epstein, M.L., 2007. Behavior of enteric neural crest-derived cells varies with respect to the migratory wavefront. Dev. Dyn. 236 (1), 84–92. http://dx.doi.org/10.1002/dvdy.20974, PubMed PMID: 17039523.

Delalande, J.M., Natarajan, D., Vernay, B., Finlay, M., Ruhrberg, C., Thapar, N., Burns, A.J., 2014. Vascularisation is not necessary for gut colonisation by enteric neural crest cells. Dev. Biol. 385 (2), 220–229. http://dx.doi.org/10.1016/j.ydbio.2013.11.007, PubMed PMID: 24262984; PMCID: PMC3928993.

Erickson, C.A., 1985. Control of neural crest cell dispersion in the trunk of the avian embryo. Dev. Biol. 111 (1), 138–157, Epub 1985/09/01. doi: 0012-1606(85)90442-7 [pii]. PubMed PMID: 4029505.

Eichmann, A., Thomas, J.L., 2013. Molecular parallels between neural and vascular development. Cold Spring Harb. Perspect. Med. 3 (1), a006551. http://dx.doi.org/10.1101/cshperspect.a006551, PubMed PMID: 23024177; PMCID: PMC3530036.

Erskine, L., Reijntjes, S., Pratt, T., Denti, L., Schwarz, Q., Vieira, J.M., Alakakone, B., Shewan, D., Ruhrberg, C., 2011. VEGF signaling through neuropilin 1 guides commissural axon crossing at the optic chiasm. Neuron 70 (5), 951–965. http://dx.doi.org/10.1016/j.neuron.2011.02.052, PubMed PMID: 21658587; PMCID: PMC3114076.

Erickson, C.A., Duong, T.D., Tosney, K.W., 1992. Descriptive and experimental analysis of the dispersion of neural crest cells along the dorsolateral path and their entry into ectoderm in the chick embryo. Dev. Biol. 151 (1), 251–272, PubMed PMID: 1577191.

Erickson, C.A., Goins, T.L., 1995. Avian neural crest cells can migrate in the dorsolateral path only if they are specified as melanocytes. Development 121 (3), 915–924, PubMed PMID: 7720593.

Ebner Vv, 1888. Urwirbel und Neugliederung der Wirbelsäule.

Etchevers, H.C., Vincent, C., Le Douarin, N.M., Couly, G.F., 2001. The cephalic neural crest provides pericytes and smooth muscle cells to all blood vessels of the face and forebrain. Development 128 (7), 1059–1068, Epub 2001/03/14. PubMed PMID: 11245571.

Fujita, M., Cha, Y.R., Pham, V.N., Sakurai, A., Roman, B.L., Gutkind, J.S., Weinstein, B. M., 2011. Assembly and patterning of the vascular network of the vertebrate hindbrain. Development 138 (9), 1705–1715. http://dx.doi.org/10.1242/dev.058776, PubMed PMID: 21429985; PMCID: PMC3074447.

Fortuna, V., Pardanaud, L., Brunet, I., Ola, R., Ristori, E., Santoro, M.M., Nicoli, S., Eichmann, A., 2015. Vascular mural cells promote noradrenergic differentiation of embryonic sympathetic neurons. Cell Rep. 11 (11), 1786–1796. http://dx.doi.org/10.1016/j.celrep.2015.05.028, PubMed PMID: 26074079.

George, L., Chaverra, M., Todd, V., Lansford, R., Lefcort, F., 2007. Nociceptive sensory neurons derive from contralaterally migrating, fate-restricted neural crest cells. Nat. Neurosci. 10 (10), 1287–1293, Epub 2007/09/11. doi: nn1962 [pii] 10.1038/nn1962. PubMed PMID: 17828258.

George, L., Kasemeier-Kulesa, J., Nelson, B.R., Koyano-Nakagawa, N., Lefcort, F., 2010. Patterned assembly and neurogenesis in the chick dorsal root ganglion. J Comp. Neurol. 518 (4), 405–422. http://dx.doi.org/10.1002/cne.22248, PubMed PMID: 20017208; PMCID: 2892853.

Gammill, L.S., Gonzalez, C., Gu, C., Bronner-Fraser, M., 2006. Guidance of trunk neural crest migration requires neuropilin 2/semaphorin 3F signaling. Development 133 (1), 99–106, Epub 2005/12/02. doi: dev.02187 [pii] 10.1242/dev.02187. PubMed PMID: 16319111.

Gelfand, M.V., Hong, S., Gu, C., 2009. Guidance from above: common cues direct distinct signaling outcomes in vascular and neural patterning. Trends Cell. Biol. 19 (3), 99–110. http://dx.doi.org/10.1016/j.tcb.2009.01.001, PubMed PMID: 19200729; PMCID: PMC3654375.

Goldman, S.A., Chen, Z., 2011. Perivascular instruction of cell genesis and fate in the adult brain. Nat. Neurosci. 14 (11), 1382–1389. http://dx.doi.org/10.1038/nn.2963, PubMed PMID: 22030549; PMCID: PMC3655803.

Gu, C., Yoshida, Y., Livet, J., Reimert, D.V., Mann, F., Merte, J., Henderson, C.E., Jessell, T.M., Kolodkin, A.L., Ginty, D.D., 2005. Semaphorin 3E and plexin-D1 control vascular pattern independently of neuropilins. Science 307 (5707), 265–268. http://dx.doi.org/10.1126/science.1105436, PubMed PMID: 15550623.

Gore, A.V., Monzo, K., Cha, Y.R., Pan, W., Weinstein, B.M., 2012. Vascular development in the zebrafish. Cold Spring Harb. Perspect. Med. 2 (5), a006684. http://dx.doi.org/10.1101/cshperspect.a006684, PubMed PMID: 22553495; PMCID: PMC3331685.

Haigh, J.J., Ema, M., Haigh, K., Gertsenstein, M., Greer, P., Rossant, J., Nagy, A., Wagner, E.F., 2004. Activated Fps/Fes partially rescues the in vivo developmental potential of Flk1-deficient vascular progenitor cells. Blood 103 (3), 912–920. http://dx.doi.org/10.1182/blood-2003-07-2343, PubMed PMID: 14552765.

Hashimoto, T., Zhang, X.M., Chen, B.Y., Yang, X.J., 2006. VEGF activates divergent intracellular signaling components to regulate retinal progenitor cell proliferation and neuronal differentiation. Development 133 (11), 2201–2210. http://dx.doi.org/10.1242/dev.02385, PubMed PMID: 16672338.

Herzog, Y., Kalcheim, C., Kahane, N., Reshef, R., Neufeld, G., 2001. Differential expression of neuropilin-1 and neuropilin-2 in arteries and veins. Mech. Dev. 109 (1), 115–119, PubMed PMID: 11677062.

Hamburger, V., Hamilton, H.L., 1992. A series of normal stages in the development of the chick embryo. 1951. Dev. Dyn. 195 (4), 231–272. http://dx.doi.org/10.1002/aja.1001950404, PubMed PMID: 1304821.

Isogai, S., Horiguchi, M., Weinstein, B.M., 2001. The vascular anatomy of the developing zebrafish: an atlas of embryonic and early larval development. Dev. Biol. 230 (2), 278–301. http://dx.doi.org/10.1006/dbio.2000.9995, PubMed PMID: 11161578.

Jesuthasan, S., 1996. Contact inhibition/collapse and pathfinding of neural crest cells in the zebrafish trunk. Development 122 (1), 381–389, Epub 1996/01/01. PubMed PMID: 8565850.

Jiang, X., Rowitch, D.H., Soriano, P., McMahon, A.P., Sucov, H.M., 2000. Fate of the mammalian cardiac neural crest. Development 127 (8), 1607–1616, PubMed PMID: 10725237.

Kasemeier-Kulesa, J.C., McLennan, R., Romine, M.H., Kulesa, P.M., Lefcort, F., 2010. CXCR4 controls ventral migration of sympathetic precursor cells. J Neurosci. 30 (39), 13078–13088, Epub 2010/10/01. doi: 30/39/13078 [pii] 10.1523/JNEUROSCI.0892-10.2010. PubMed PMID: 20881125.

Krull, C.E., Lansford, R., Gale, N.W., Collazo, A., Marcelle, C., Yancopoulos, G.D., Fraser, S.E., Bronner-Fraser, M., 1997. Interactions of Eph-related receptors and ligands confer rostrocaudal pattern to trunk neural crest migration. Curr. Biol. 7 (8), 571–580, PubMed PMID: 9259560.

Kasemeier-Kulesa, J.C., Bradley, R., Pasquale, E.B., Lefcort, F., Kulesa, P.M., 2006. Eph/ephrins and N-cadherin coordinate to control the pattern of sympathetic ganglia. Development 133 (24), 4839–4847, Epub 2006/11/17. doi: dev.02662 [pii] 10.1242/dev.02662. PubMed PMID: 17108003.

Kasemeier-Kulesa, J.C., Kulesa, P.M., Lefcort, F., 2005. Imaging neural crest cell dynamics during formation of dorsal root ganglia and sympathetic ganglia. Development 132 (2), 235–245, Epub 2004/12/14. doi: dev.01553 [pii] 10.1242/dev.01553. PubMed PMID: 15590743.

Krull, C.E., Collazo, A., Fraser, S.E., Bronner-Fraser, M., 1995. Segmental migration of trunk neural crest: time-lapse analysis reveals a role for PNA-binding molecules. Development 121 (11), 3733–3743, Epub 1995/11/01. PubMed PMID: 8582285.

Kulesa, P.M., Fraser, S.E., 1998. Neural crest cell dynamics revealed by time-lapse video microscopy of whole embryo chick explant cultures. Dev. Biol. 204 (2), 327–344, Epub 1999/01/12. doi: S0012-1606(98)99082-0 [pii] 10.1006/dbio.1998.9082. PubMed PMID: 9882474.

Kulesa, P.M., Lefcort, F., Kasemeier-Kulesa, J.C., 2009. The migration of autonomic precursor cells in the embryo. Auton. Neurosci.: Basic Clin. 151 (1), 3–9. http://dx.doi.org/10.1016/j.autneu.2009.08.013, PubMed PMID: 19783486.

Kulesa, P.M., Morrison, J.A., Bailey, C.M., 2013. The neural crest and cancer: a developmental spin on melanoma. Cells Tissues Organs 198 (1), 12–21. http://dx.doi.org/10.1159/000348418, PubMed PMID: 23774755; PMCID: PMC3809092.

Kulesa, P.M., Teddy, J.M., Stark, D.A., Smith, S.E., McLennan, R., 2008. Neural crest invasion is a spatially-ordered progression into the head with higher cell proliferation at the migratory front as revealed by the photoactivatable protein, KikGR. Dev. Biol. 316 (2), 275–287, Epub 2008/03/11. doi: S0012-1606(08)00064-X [pii] 10.1016/j.ydbio.2008.01.029. PubMed PMID: 18328476; PMCID: 3501347.

Kalcheim, C., Goldstein, R.S., 1991. Segmentation of sensory and sympathetic ganglia: interactions between neural crest and somite cells. J. Physiol. (Paris) 85 (3), 110–116, PubMed PMID: 1818106.

Keynes, R.J., Stern, C.D., 1984. Segmentation in the vertebrate nervous system. Nature 310 (5980), 786–789, PubMed PMID: 6472458.

Lallier, T.E., Bronner-Fraser, M., 1988. A spatial and temporal analysis of dorsal root and sympathetic ganglion formation in the avian embryo. Dev. Biol. 127 (1), 99–112, Epub 1988/05/01. doi: 0012-1606(88)90192-3 [pii]. PubMed PMID: 3282919.

Le Douarin, N.M., Kalcheim, C., 1999. The Neural Crest, 2nd ed. Cambridge University Press, p. 445.

Loring, J.F., Erickson, C.A., 1987. Neural crest cell migratory pathways in the trunk of the chick embryo. Dev. Biol. 121 (1), 220–236, Epub 1987/05/01. doi: 0012-1606(87)90154-0 [pii]. PubMed PMID: 3552788.

Langenberg, T., Kahana, A., Wszalek, J.A., Halloran, M.C., 2008. The eye organizes neural crest cell migration. Dev. Dyn. 237 (6), 1645–1652. http://dx.doi.org/10.1002/dvdy.21577, PubMed PMID: 18498099; PMCID: 2762319.

Landman, K.A., Fernando, A.E., Zhang, D., Newgreen, D.F., 2011. Building stable chains with motile agents: Insights into the morphology of enteric neural crest cell migration. J. Theor. Biol. 276 (1), 250–268. http://dx.doi.org/10.1016/j.jtbi.2011.01.043, PubMed PMID: 21296089.

Le Bras, B., Barallobre, M.J., Homman-Ludiye, J., Ny, A., Wyns, S., Tammela, T., Haiko, P., Karkkainen, M.J., Yuan, L., Muriel, M.P., Chatzopoulou, E., Breant, C., Zalc, B., Carmeliet, P., Alitalo, K., Eichmann, A., Thomas, J.L., 2006. VEGF-C is a trophic factor for neural progenitors in the vertebrate embryonic brain. Nat. Neurosci. 9 (3), 340–348. http://dx.doi.org/10.1038/nn1646, PubMed PMID: 16462734.

Lichtman, J.W., Fraser, S.E., 2001. The neuronal naturalist: watching neurons in their native habitat. Nat. Neurosci. 4 (Suppl.), S1215–S1220. http://dx.doi.org/10.1038/nn754, PubMed PMID: 11687832.

Li, L., Fukunaga-Kalabis, M., Herlyn, M., 2013. Isolation, characterization, and differentiation of human multipotent dermal stem cells. Methods Mol. Biol. 989,

235–246. http://dx.doi.org/10.1007/978-1-62703-330-5_18, PubMed PMID: 23483399.

Liang, D., Wang, X., Mittal, A., Dhiman, S., Hou, S.Y., Degenhardt, K., Astrof, S., 2014. Mesodermal expression of integrin alpha5beta1 regulates neural crest development and cardiovascular morphogenesis. Dev. Biol. 395 (2), 232–244. http://dx.doi.org/10.1016/j.ydbio.2014.09.014, PubMed PMID: 25242040; PMCID: PMC4252364.

Miller, L.C., Freter, S., Liu, F., Taylor, J.S., Patient, R., Begbie, J., 2010. Separating early sensory neuron and blood vessel patterning. Dev. Dyn. 239 (12), 3297–3302. http://dx.doi.org/10.1002/dvdy.22464, PubMed PMID: 21061240.

Martin, P., Lewis, J., 1989. Origins of the neurovascular bundle: interactions between developing nerves and blood vessels in embryonic chick skin. Int. J. Dev. Biol. 33 (3), 379–387, PubMed PMID: 2702122.

Mukouyama, Y.S., Shin, D., Britsch, S., Taniguchi, M., Anderson, D.J., 2002. Sensory nerves determine the pattern of arterial differentiation and blood vessel branching in the skin. Cell 109 (6), 693–705, PubMed PMID: 12086669.

Makita, T., Sucov, H.M., Gariepy, C.E., Yanagisawa, M., Ginty, D.D., 2008. Endothelins are vascular-derived axonal guidance cues for developing sympathetic neurons. Nature 452 (7188), 759–763. http://dx.doi.org/10.1038/nature06859, PubMed PMID: 18401410; PMCID: PMC2713667.

Mukouyama, Y.S., Gerber, H.P., Ferrara, N., Gu, C., Anderson, D.J., 2005. Peripheral nerve-derived VEGF promotes arterial differentiation via neuropilin 1-mediated positive feedback. Development 132 (5), 941–952. http://dx.doi.org/10.1242/dev.01675, PubMed PMID: 15673567.

MacDonald, G.H., Rubel, E.W., 2008. Three-dimensional imaging of the intact mouse cochlea by fluorescent laser scanning confocal microscopy. Hear. Res. 243 (1–2), 1–10. http://dx.doi.org/10.1016/j.heares.2008.05.009, PubMed PMID: 18573326; PMCID: PMC2566306.

Ma, Q., Fode, C., Guillemot, F., Anderson, D.J., 1999. Neurogenin1 and neurogenin2 control two distinct waves of neurogenesis in developing dorsal root ganglia. Genes. Dev. 13 (13), 1717–1728, Epub 1999/07/10. PubMed PMID: 10398684; PMCID: 316844.

Marmigere, F., Ernfors, P., 2007. Specification and connectivity of neuronal subtypes in the sensory lineage. Nat. Rev. Neurosci. 8 (2), 114–127, Epub 2007/01/24. doi: nrn2057 [pii] 10.1038/nrn2057. PubMed PMID: 17237804.

Milgrom-Hoffman, M., Michailovici, I., Ferrara, N., Zelzer, E., Tzahor, E., 2014. Endothelial cells regulate neural crest and second heart field morphogenesis. Biol. Open 3 (8), 679–688. http://dx.doi.org/10.1242/bio.20148078, PubMed PMID: 24996922; PMCID: PMC4133721.

Newgreen, D.F., Powell, M.E., Moser, B., 1990. Spatiotemporal changes in HNK-1/L2 glycoconjugates on avian embryo somite and neural crest cells. Dev. Biol. 139 (1), 100–120, PubMed PMID: 1691722.

Nagy, N., Mwizerwa, O., Yaniv, K., Carmel, L., Pieretti-Vanmarcke, R., Weinstein, B. M., Goldstein, A.M., 2009. Endothelial cells promote migration and proliferation of enteric neural crest cells via beta1 integrin signaling. Dev. Biol. 330 (2), 263–272. http://dx.doi.org/10.1016/j.ydbio.2009.03.025, PubMed PMID: 19345201; PMCID: PMC2690696.

Pan, Q., Chathery, Y., Wu, Y., Rathore, N., Tong, R.K., Peale, F., Bagri, A., Tessier-Lavigne, M., Koch, A.W., Watts, R.J., 2007. Neuropilin-1 binds to VEGF121 and regulates endothelial cell migration and sprouting. J. Biol. Chem. 282 (33), 24049–24056. http://dx.doi.org/10.1074/jbc.M703554200, PubMed PMID: 17575273.

Poynter, G., Lansford, R., 2008. Generating transgenic quail using lentiviruses. Methods Cell. Biol. 87, 281–293, Epub 2008/05/20. doi: S0091-679X(08)00215-X [pii] 10.1016/S0091-679X(08)00215-X. PubMed PMID: 18485303.

Plein, A., Calmont, A., Fantin, A., Denti, L., Anderson, N.A., Scambler, P.J., Ruhrberg, C., 2015. Neural crest-derived SEMA3C activates endothelial NRP1 for cardiac outflow tract septation. J. Clin. Investig. 125 (7), 2661–2676. http://dx.doi.org/10.1172/JCI79668, PubMed PMID: 26053665.

Quaegebeur, A., Lange, C., Carmeliet, P., 2011. The neurovascular link in health and disease: molecular mechanisms and therapeutic implications. Neuron. 71 (3), 406–424. http://dx.doi.org/10.1016/j.neuron.2011.07.013, PubMed PMID: 21835339.

Rupp, P.A., Filla, M.B., Cui, C., Little, C.D., 2008. Chapter 5. Avian embryos a model for the study of primary vascular assembly in warm-blooded animals. Methods Enzymol. 445, 107–123. http://dx.doi.org/10.1016/S0076-6879(08)03005-X, PubMed PMID: 19022057.

Rupp, P.A., Czirok, A., Little, C.D., 2004. alphavbeta3 integrin-dependent endothelial cell dynamics in vivo. Development 131 (12), 2887–2897. http://dx.doi.org/10.1242/dev.01160, PubMed PMID: 15151986.

Rupp, P.A., Rongish, B.J., Czirok, A., Little, C.D., 2003. Culturing of avian embryos for time-lapse imaging. Biotechniques 34 (2), 274–278, PubMed PMID: 12613250.

Rawles, M.E., 1948. Origin of melanophores and their role in development of color patterns in vertebrates. Physiol. Rev. 28 (4), 383–408, PubMed PMID: 18894955.

Rifkin, J.T., Todd, V.J., Anderson, L.W., Lefcort, F., 2000. Dynamic expression of neurotrophin receptors during sensory neuron genesis and differentiation. Dev. Biol. 227 (2), 465–480. http://dx.doi.org/10.1006/dbio.2000.9841, S0012-1606 (00)99841-5 [pii]. PubMed PMID: 11071767.

Reissmann, E., Reissmann, U., Francis-West, P.H., Rueger, D., Brickell, P.M., Rohrer, H., 1996. Involvement of bone morphogenetic protein-4 and bone morphogenetic protein-7 in the differentiation of the adrenergic phenotype in developing sympathetic neurons. Development 122 (7), 2079–2088, PubMed PMID: 8681789.

Schwarz, Q., Maden, C.H., Vieira, J.M., Ruhrberg, C., 2009. Neuropilin 1 signaling guides neural crest cells to coordinate pathway choice with cell specification. Proc. Natl. Acad. Sci. USA 106 (15), 6164–6169, Epub 2009/03/28. doi:

0811521106 [pii] 10.1073/pnas.0811521106. PubMed PMID: 19325129; PMCID: 2661313.

Saito, D., Takase, Y., Murai, H., Takahashi, Y., 2012. The dorsal aorta initiates a molecular cascade that instructs sympatho-adrenal specification. Science 336 (6088), 1578–1581. http://dx.doi.org/10.1126/science.1222369, PubMed PMID: 22723422.

Spence, S.G., Poole, T.J., 1994. Developing blood vessels and associated extracellular matrix as substrates for neural crest migration in Japanese quail, Coturnix coturnix japonica. Int. J Dev. Biol. 38 (1), 85–98, PubMed PMID: 7521199.

Suchting, S., Heal, P., Tahtis, K., Stewart, L.M., Bicknell, R., 2005. Soluble Robo4 receptor inhibits in vivo angiogenesis and endothelial cell migration. FASEB J. 19 (1), 121–123. http://dx.doi.org/10.1096/fj.04-1991fje, PubMed PMID: 15486058.

Saghatelyan, A., 2009. Role of blood vessels in the neuronal migration. Semin. Cell. Dev. Biol. 20 (6), 744–750. http://dx.doi.org/10.1016/j.semcdb.2009.04.006, PubMed PMID: 19374951.

Snapyan, M., Lemasson, M., Brill, M.S., Blais, M., Massouh, M., Ninkovic, J., Gravel, C., Berthod, F., Gotz, M., Barker, P.A., Parent, A., Saghatelyan, A., 2009. Vasculature guides migrating neuronal precursors in the adult mammalian forebrain via brain-derived neurotrophic factor signaling. J. Neurosci. 29 (13), 4172–4188. http://dx.doi.org/10.1523/JNEUROSCI.4956-08.2009, PubMed PMID: 19339612.

Sondell, M., Lundborg, G., Kanje, M., 1999. Vascular endothelial growth factor has neurotrophic activity and stimulates axonal outgrowth, enhancing cell survival and Schwann cell proliferation in the peripheral nervous system. J. Neurosci. 19 (14), 5731–5740, PubMed PMID: 10407014.

Suchting, S., Freitas, C., le Noble, F., Benedito, R., Breant, C., Duarte, A., Eichmann, A., 2007. The Notch ligand Delta-like 4 negatively regulates endothelial tip cell formation and vessel branching. Proc. Natl. Acad. Sci. USA 104 (9), 3225–3230. http://dx.doi.org/10.1073/pnas.0611177104, PubMed PMID: 17296941; PMCID: PMC1805603.

Shen, Q., Goderie, S.K., Jin, L., Karanth, N., Sun, Y., Abramova, N., Vincent, P., Pumiglia, K., Temple, S., 2004. Endothelial cells stimulate self-renewal and expand neurogenesis of neural stem cells. Science 304 (5675), 1338–1340. http://dx.doi.org/10.1126/science.1095505, PubMed PMID: 15060285.

Sato, Y., Poynter, G., Huss, D., Filla, M.B., Czirok, A., Rongish, B.J., Little, C.D., Fraser, S. E., Lansford, R., 2010. Dynamic analysis of vascular morphogenesis using transgenic quail embryos. PLoS One 5 (9), e12674. http://dx.doi.org/10.1371/journal.pone.0012674, PMCID: PMC2939056.

Shaner, N.C., Campbell, R.E., Steinbach, P.A., Giepmans, B.N., Palmer, A.E., Tsien, R.Y., 2004. Improved monomeric red, orange and yellow fluorescent proteins derived from Discosoma sp. red fluorescent protein. Nat. Biotechnol. 22 (12), 1567–1572. http://dx.doi.org/10.1038/nbt1037, PubMed PMID: 15558047.

Seidl, A.H., Sanchez, J.T., Schecterson, L., Tabor, K.M., Wang, Y., Kashima, D.T., Poynter, G., Huss, D., Fraser, S.E., Lansford, R., Rubel, E.W., 2013. Transgenic quail as a model for research in the avian nervous system: a comparative study of the auditory brainstem. J. Comp. Neurol. 521 (1), 5–23. http://dx.doi.org/10.1002/cne.23187, PubMed PMID: 22806400; PMCID: PMC3488602.

Stainier, D.Y., Weinstein, B.M., Detrich 3rd, H.W., Zon, L.I., Fishman, M.C., 1995. Cloche, an early acting zebrafish gene, is required by both the endothelial and hematopoietic lineages. Development 121 (10), 3141–3150, PubMed PMID: 7588049.

Santiago, A., Erickson, C.A., 2002. Ephrin-B ligands play a dual role in the control of neural crest cell migration. Development 129 (15), 3621–3632, PubMed PMID: 12117812.

Tosney, K.W., 1978. The early migration of neural crest cells in the trunk region of the avian embryo: an electron microscopic study. Dev. Biol. 62 (2), 317–333, Epub 1978/02/01. doi: 0012-1606(78)90219-1 [pii]. PubMed PMID: 627310.

Thiery, J.P., Duband, J.L., Delouvee, A., 1982. Pathways and mechanisms of avian trunk neural crest cell migration and localization. Dev. Biol. 93 (2), 324–343, PubMed PMID: 7141101.

Teillet, M.A., Kalcheim, C., Le Douarin, N.M., 1987. Formation of the dorsal root ganglia in the avian embryo: segmental origin and migratory behavior of neural crest progenitor cells. Dev. Biol. 120 (2), 329–347, PubMed PMID: 3549390.

Teddy, J.M., Kulesa, P.M., 2004. In vivo evidence for short- and long-range cell communication in cranial neural crest cells. Development 131 (24), 6141–6151. http://dx.doi.org/10.1242/dev.01534, PubMed PMID: 15548586.

Taylor, G.I., Gianoutsos, M.P., Morris, S.F., 1994. The neurovascular territories of the skin and muscles: anatomic study and clinical implications. Plast. Reconstr. Surg. 94 (1), 1–36, PubMed PMID: 8016221.

Taipale, J., Keski-Oja, J., 1997. Growth factors in the extracellular matrix. FASEB J. 11 (1), 51–59, PubMed PMID: 9034166.

Thiery, J.-P., Duband, J.L., 1986. Role of tissue environment and fibronectin in the patterning of neural crest derivatives. Trends Neurosci. 9, 565–570.

Thiery, J.P., Duband, J.L., Tucker, G.C., 1985. Cell migration in the vertebrate embryo: role of cell adhesion and tissue environment in pattern formation. Annu. Rev. Cell. Biol. 1, 91–113. http://dx.doi.org/10.1146/annurev.cb.01.110185.000515, PubMed PMID: 3916324.

Vesalius A. De humani corporis fabrica libri septem1543.

Vieira, J.M., Schwarz, Q., Ruhrberg, C., 2007. Role of the neuropilin ligands VEGF164 and SEMA3A in neuronal and vascular patterning in the mouse. Novartis Found. Symp. 283, 230–235, discussion 5-41. PubMed PMID: 18300426; PMCID: PMC2953635.

Weston, J.A., 1970. The migration and differentiation of neural crest cells. Adv. Morphog. 8, 41–114, Epub 1970/01/01. PubMed PMID: 4906187.

Weston, J.A., 1991. Sequential segregation and fate of developmentally restricted intermediate cell populations in the neural crest lineage. Curr. Top Dev. Biol. 25, 133–153, PubMed PMID: 1660392.

Weinstein, B.M., 2005. Vessels and nerves: marching to the same tune. Cell 120 (3), 299–302. http://dx.doi.org/10.1016/j.cell.2005.01.010, PubMed PMID: 15707889.

Wilting, J., Brand-Saberi, B., Huang, R., Zhi, Q., Kontges, G., Ordahl, C.P., Christ, B., 1995. Angiogenic potential of the avian somite. Dev. Dyn. 202 (2), 165–171. http://dx.doi.org/10.1002/aja.1002020208, PubMed PMID: 7537553.

Wakamatsu, Y., Maynard, T.M., Weston, J.A., 2000. Fate determination of neural crest cells by NOTCH-mediated lateral inhibition and asymmetrical cell division during gangliogenesis. Development 127 (13), 2811–2821, PubMed PMID: 10851127.

Wang, H.U., Anderson, D.J., 1997. Eph family transmembrane ligands can mediate repulsive guidance of trunk neural crest migration and motor axon outgrowth. Neuron 18 (3), 383–396, PubMed PMID: 9115733.

Wiszniak, S., Mackenzie, F.E., Anderson, P., Kabbara, S., Ruhrberg, C., Schwarz, Q., 2015. Neural crest cell-derived VEGF promotes embryonic jaw extension. Proc. Natl. Acad. Sci. USA 112 (19), 6086–6091. http://dx.doi.org/10.1073/pnas.1419368112, PubMed PMID: 25922531; PMCID: PMC4434710.

Young, H.M., Bergner, A.J., Anderson, R.B., Enomoto, H., Milbrandt, J., Newgreen, D. F., Whitington, P.M., 2004. Dynamics of neural crest-derived cell migration in the embryonic mouse gut. Dev. Biol. 270 (2), 455–473. http://dx.doi.org/10.1016/j.ydbio.2004.03.015, S0012160604002027 [pii]. PubMed PMID: 15183726.

Zacchigna, S., Pattarini, L., Zentilin, L., Moimas, S., Carrer, A., Sinigaglia, M., Arsic, N., Tafuro, S., Sinagra, G., Giacca, M., 2008. Bone marrow cells recruited through the neuropilin-1 receptor promote arterial formation at the sites of adult neoangiogenesis in mice. J. Clin. Investig. 118 (6), 2062–2075. http://dx.doi.org/10.1172/JCI32832, PubMed PMID: 18483621; PMCID: PMC2381745.

Zacchigna, S., Lambrechts, D., Carmeliet, P., 2008. Neurovascular signalling defects in neurodegeneration. Nat. Rev. Neurosci. 9 (3), 169–181. http://dx.doi.org/10.1038/nrn2336, PubMed PMID: 18253131.